



The postcranial anatomy of *Diademodon tetragonus* (Cynodontia, Cynognathia)

Leandro C. Gaetano, Helke Mocke & Fernando Abdala

To cite this article: Leandro C. Gaetano, Helke Mocke & Fernando Abdala (2018): The postcranial anatomy of *Diademodon tetragonus* (Cynodontia, Cynognathia), *Journal of Vertebrate Paleontology*, DOI: [10.1080/02724634.2018.1451872](https://doi.org/10.1080/02724634.2018.1451872)

To link to this article: <https://doi.org/10.1080/02724634.2018.1451872>



Published online: 30 Apr 2018.



Submit your article to this journal [↗](#)



View related articles [↗](#)



View Crossmark data [↗](#)

THE POSTCRANIAL ANATOMY OF *DIADEMODON TETRAGONUS* (CYNODONTIA, CYNOGNATHIA)

LEANDRO C. GAETANO,*^{1,2} HELKE MOCKE,³ and FERNANDO ABDALA^{2,4}

¹Departamento de Ciencias Geológicas, Facultad de Ciencias Exactas y Naturales, Instituto de Estudios Andinos 'Don Pablo Groeber,' IDEAN (Universidad de Buenos Aires, CONICET), Intendente Güiraldes 2160, Ciudad Universitaria-Pabellón II, C1428EGA, Ciudad Autónoma de Buenos Aires, Argentina, lcgatano@gl.fcen.uba.ar;

²Evolutionary Studies Institute, University of the Witwatersrand, Private Bag 3, WITS 2050, Johannesburg, South Africa;

³Geological Survey of Namibia, Private Bag 13297, Windhoek, Namibia, Helke.Mocke@mme.gov.na;

⁴Unidad Ejecutora Lillo, CONICET-Fundación Miguel Lillo, Miguel Lillo 251, 4000, San Miguel de Tucumán, Tucumán, Argentina, lviutiabdala2@gmail.com

ABSTRACT—A survey of the postcranial anatomy of a specimen of *Diademodon tetragonus* recovered from the Upper Omingonde Formation in Namibia resulted in the recognition of diagnostic characters in the axis, scapula, interclavicle, manubrium, sternebrae, humerus, ilium, ischium, and femur. Our comparative analysis shows that these and other postcranial features distinguish *Diademodon tetragonus* from other cynognathians. The presence of ossified sternal elements (manubrium and sternebrae) in *Diademodon tetragonus* stands out because they are otherwise only present in tritylodontids among non-mammaliaform cynodonts. It is suggested that this feature is not linked to body size but could be phylogenetically informative. A review of the postcranial anatomy of specimens previously identified as *Diademodon* and ?*Cynognathus*? *Diademodon* shows that only a few of them can be assigned to *Diademodon tetragonus*.

Citation for this article: Gaetano, L. C., H. Mocke, and F. Abdala. 2018. The postcranial anatomy of *Diademodon tetragonus* (Cynodontia, Cynognathia). *Journal of Vertebrate Paleontology*. DOI: 10.1080/02724634.2018.1451872.

INTRODUCTION

Diademodon is a relatively large cynognathian cynodont with a wide geographic distribution. It has been recorded in the Río Seco de la Quebrada Formation (Argentina), the Upper Omingonde Formation (Namibia), the Burgersdorp Formation (South Africa), the Manda Beds (Tanzania), and the lower Ntawere Formation (Zambia) (Crompton, 1955; Brink, 1963; Keyser, 1973a, 1973b; Martinelli et al., 2009). This taxon is one of the main components of the B subzone and also represented in the C subzone (Smith et al., 2012) of the *Cynognathus* Assemblage Zone (AZ) defined for Middle Triassic (Anisian) African localities (e.g., Kitching, 1995) and has been key for the recognition of this assemblage zone in South America, particularly in western Argentina (Martinelli et al., 2009). However, recent high-precision geochronological dating suggests that the Argentinean *Diademodon*-bearing levels are from the Late Triassic (early Carnian), at least 10 million years younger than the putative age usually attributed to the African *Cynognathus* AZ (Ottone et al., 2014; see also Martinelli et al., 2017). Mainly known through cranial remains (Hopson and Kitching, 1972; Brink, 1979; Martinelli et al., 2009), *Diademodon* is one of the earliest cynodonts with craniomandibular features indicating the presence of rudimentary occlusion among postcanines (Crompton, 1972; Grine, 1977).

Although several species of *Diademodon* have been recognized in the past, *Diademodon tetragonus* Seeley, 1894, is the only species considered valid to date (Grine, 1978, 1981; Grine and Hahn, 1978; Grine et al., 1978; Bradu and Grine, 1979; Martinelli et al.,

2009). Like most basal cynodonts, *Diademodon* is recognized on the basis of cranial and dental elements (e.g., Seeley, 1895a; Martinelli et al., 2009). On the other hand, the taxonomic identification of postcranial elements that are not unquestionably associated to cranial remains is to date impossible (Jenkins, 1971).

Several papers on the anatomy, taxonomy, phylogeny, histology, paleoecology, and biostratigraphic distribution of *Diademodon* have been published (e.g., Seeley, 1894, 1895a; Broom, 1911, 1919; Watson, 1911, 1913; Broili and Schröder, 1935; Brink, 1955, 1956, 1963; Fourie, 1963; Hopson, 1971; Crompton, 1972; Osborn, 1974; Grine, 1977; Grine and Hahn, 1978; Grine et al., 1978, 1979; Kitching, 1995; Botha and Chinsamy, 2000; Abdala et al., 2005; Botha et al., 2005; Martinelli et al., 2009; Liu and Olsen, 2010; Liu and Abdala, 2014; Ottone et al., 2014). Due to the relevance of *Diademodon*, many researchers have attempted to analyze its postcranial anatomy; however, the taxonomic assignation is not certain for most of the studied specimens (e.g., Brink, 1955; Jenkins, 1971). At present, only two specimens include reasonably well represented postcranial remains that can be unambiguously assigned to *Diademodon*. One of them, USNM V23352, includes a relatively complete axial skeleton that provides very little information (Jenkins, 1971). The second one (SAM-PK-K5266) is a partially preserved, small, articulated skeleton, with many of the bones only preserved as natural molds (Gow and Grine, 1979). Two further *Diademodon* specimens (AM 458 and SAM-PK-K4002) are only represented by very scarce postcranial elements (Broom, 1903; Abdala, 1999). In addition, except for the monographic work of Jenkins (1971), the published descriptions are only superficial and are not properly illustrated.

Herein, we describe in detail, for the first time, an almost complete postcranium unquestionably associated with cranial

*Corresponding author.

Color versions of one or more of the figures in the article can be found online at www.tandfonline.com/ujvp.

remains of *Diademodon tetragonus* from the Middle Triassic Omingonde Formation in Namibia.

GEOLOGICAL BACKGROUND

Triassic sediments of the Omingonde Formation accumulated in a southwest-northeast trending rift basin, the Waterberg Basin, which is located in northwestern Namibia and positioned next to an active fault margin, known as the Waterberg-Omaruru Fault Zone (Smith and Swart, 2002). Holzförster et al. (1999) subdivided the Omingonde Formation into four units, each composed of sets of related depositional cycles separated by erosional or sediment bypass contacts. The Upper Omingonde Formation corresponds to the last two upper units. According to Holzförster et al. (1999) and Wanke (2000), the Upper Omingonde Formation was deposited gradually as a result of a progressive change in environmental and climatic conditions during which there was a switch from a braided river system in a semiarid climate to a more meandering river system with decreasing discharge rates in a wetter environment. Smith and Swart (2002) proposed a similar change in environments, from a single, wide, shallow braided system to a narrow series of meander belts separated by floodplains. According to Smith and Swart (2002), this change took place over a period of about 5 million years. They recognized three sedimentological facies associations within the Upper Omingonde Formation: (1) loessic plains with saline lakes and ponds, (2) gravel bed meandering rivers on semiarid floodplains, and (3) sand bed meandering streams on semiarid loessic plains with saline ponds. Fossils were discovered in the loessic mudrocks.

Abdala and Smith (2009) noted that the stratigraphic position of Keyser's three arenaceous horizons and the fossils he collected in relation to these are not well defined and that the stratigraphic schemes used by Smith and Swart (2002) and Holzförster et al. (1999) do not match Keyser's (1973a, 1973b) scheme. According to Keyser (1973a, 1973b), the *Diademodon tetragonus* specimen (GSN R327) described here was found at the western buttress of Etjo Mountain in the nodule-bearing shale beds between two arenaceous horizons. This geographic and stratigraphic provenance allows us to suggest that GSN R327 comes from the lower levels of the Upper Omingonde Formation, an interpretation consistent with the stratigraphic distribution of *Diademodon* remains in this unit as inferred by Abdala and Smith (2009).

The Upper Omingonde Formation was initially interpreted as Olenekian-Anisian in age by Keyser (1973a, 1973b, 1978) and Kitching (1995), but in recent years it has been reinterpreted as Anisian-Ladinian (Abdala and Smith, 2009; Abdala et al., 2013).

The lower and middle levels of the upper portion of the Omingonde Formation could be correlated to Subzone B of the *Cynognathus* AZ due to the presence of *Cynognathus* and *Diademodon* and may be of Anisian age (Abdala and Smith, 2009; Abdala et al., 2013; but see Ottone et al., 2014). The faunal composition of the assemblage from the uppermost levels of the unit suggests correlation with the *Dinodontosaurus* AZ of the Santa Maria Formation from Brazil and the Chañares Formation from Argentina (Abdala and Smith, 2009; Abdala et al., 2013; Martinelli et al., 2017). The absolute dates recently published for the Chañares Formation of Argentina indicate an early Carnian age for this unit (Marsicano et al., 2016); therefore, that is also the putative age considered for the fauna from the *Dinodontosaurus* AZ of the Pinheiros-Chiniqua Sequence of the Santa Maria Supersequence and the one recovered at the top of the Upper Omingonde Formation (Marsicano et al., 2016; but see Ezcurra et al., 2017).

MATERIALS AND METHODS

The specimen studied was collected by Dr. A. W. Keyser and is kept in the paleontological collections of the Geological Survey of Namibia labeled with the number GSN R327. Under this collection number, there are several individuals that belong to two taxa. One of them, a skull associated with part of the postcranial skeleton (i.e., sacral vertebrae, ilium, ischium, scapula, coracoid), is included in a single not fully prepared block and has been identified as *Trirachodon* (Keyser, 1973a). Although Keyser (1973a) acknowledged some differences with other specimens of this genus, after the thorough analysis of the remains we consider his identification to be correct.

Keyser (1973a) also reported the finding of material consisting of an almost complete skull with postcranial elements (GSN R327) that he tentatively assigned to *Diademodon tetragonus*. At present, the skull of specimen GSN R327 figured by Keyser (1973a:figs. 8–9) could not be found in the collections of the Geological Survey of Namibia. On the other hand, previously unmentioned cranial remains, which can be confidently assigned to *Diademodon tetragonus* on the basis of their morphology, are also labeled GSN R327 (Fig. 1) and are kept together with postcranial elements with the same collection number. They are represented by a fragment of the left maxilla in close contact with the left ramus of a partial lower jaw (Fig. 1A–E) and an edentulous fragment of the left lower jaw of a slightly larger individual (Fig. 1F–G). The latter fragmentary jaw matches in size the skull reported by Keyser (1973a) and could be part of the same

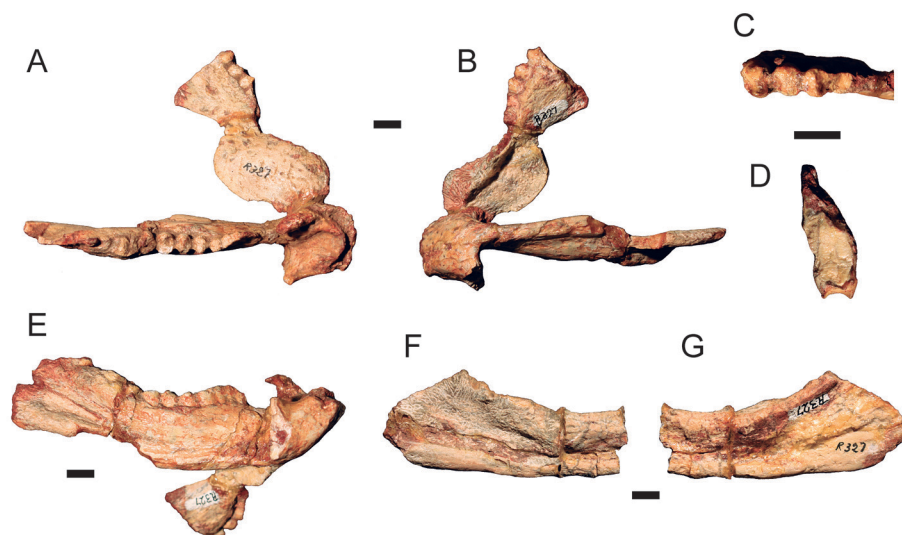


FIGURE 1. Cranial elements of *Diademodon tetragonus* (GSN R327). **A–B**, fragmentary left lower jaw and left maxilla in dorsal and lateral views (**A**) and in ventral and medial views (**B**), respectively. **C**, occlusal view of the preserved postcanine in the left maxilla fragment (anterior to the right). **D**, posterior view of the fragmentary left maxilla showing the crown of the last preserved postcanine (lateral to the left). **E**, fragmentary left lower jaw in lateral view. **F–G**, edentulous fragmentary left lower jaw in lateral (**F**) and medial (**G**) views. Scale bars equal 10 mm.

individual. Among the postcranial remains of GSN R327, there are two left femora and two right ischia. These duplicated elements are extremely similar morphologically and in size to each other and could belong to the same two individuals represented by the above-referred cranial material.

The postcranial elements of *Diademodon tetragonus* of specimen GSN R327 were preserved very close to each other, some almost semiarticulated, and others in natural connection. Hence, we conservatively assume that they belong to the same individual (A), except for those duplicated bones that must necessarily correspond to a different individual (B). In this scenario, individual A is represented by a left maxilla in close contact with the left ramus of a partial lower jaw and the following postcranial elements: atlas-axis articulated with the first three postaxial cervical vertebrae and very closely preserved (but not articulated) to the sixth and seventh cervical vertebrae; seven articulated but poorly preserved dorsal vertebrae; the complete left scapula; the partially preserved left clavicle in articulation with the almost complete interclavicle; articulated sternal elements (manubrium and the first two sternebrae); the complete right humerus; the almost complete left radius; the left ulna missing the distal portion; the partially preserved right ilium and ischium in contact with each other; the proximal portions of the right and left femora; the incomplete right fibula; a right lumbar rib; and some not very well preserved nonexpanded ribs. The second individual (B) is inferred to include three bones that are slightly larger than the corresponding elements interpreted to belong to individual A. These elements are an edentulous left lower jaw fragment; a right ischium, not preserved in contact with the right ilium; and a left femur that preserves the diaphysis and the lesser trochanter but lacks the distal portion, the femoral head, and most of the greater trochanter. All GSN R327 *Diademodon tetragonus* elements are very similarly preserved but differently from the *Trirachodon* specimen GSN R327.

Institutional Abbreviations—**AM**, Albany Museum, Grahamstown, South Africa; **BPI**, Evolutionary Studies Institute (formerly Bernard Price Institute), Johannesburg, South Africa; **DMSW**, D.M.S. Watson Collection, now housed in the University Museum of Zoology, Cambridge, England; **GSN**, Geological Survey of Namibia (National Earth Science Museum), Windhoek, Namibia; **MCZ**, Museum of Comparative Zoology, Harvard University, Massachusetts, U.S.A.; **MLP**, Museo de La Plata, La Plata, Argentina; **NHMUK**, Natural History Museum, London, U.K.; **NMB**, National Museum, Bloemfontein, South Africa; **NMQR**, National Museum, Bloemfontein, South Africa; **PVL**, Colección Sección Paleontología de Vertebrados, Instituto Miguel Lillo, Tucumán, Argentina; **SAM-PK**, Iziko South African Museum, Cape Town, South Africa; **UNIPAMPA**, Laboratorio de Paleobiología, Universidade Federal do Pampa, Rio Grande do Sul, Brasil; **USNM V**, Vertebrate Paleontology Collection at the National Museum of Natural History, Washington, D.C., U.S.A.

SYSTEMATIC PALEONTOLOGY

THERAPSIDA Broom, 1905
 CYNODONTIA Owen, 1861
 EUCYNODONTIA Kemp, 1982
 CYNOGNATHIA Hopson and Kitching, 2001
DIADEMODON TETRAGONUS Seeley, 1894
 (Figs. 1–9)

Referred Specimen—GSN R327, cranial and postcranial elements preserved very close to each other, almost semiarticulated, and/or in natural connection, of at least two individuals. Elements represented are: fragmentary left maxilla, two partial left lower jaws, atlas-axis, first five postaxial cervical vertebrae, seven articulated but poorly preserved dorsal vertebrae, left scapula, partial left clavicle, interclavicle, articulated manubrium and the two first sternebrae, right humerus, left radius, partial left ulna, incomplete right ilium and ischium in articulation, fragmentary

isolated right ischium, the proximal portion of a right and a left femur, incomplete left femur, incomplete right fibula, a right lumbar rib, and poorly preserved nonexpanded ribs.

Diagnosis—*Diademodon tetragonus* is a relatively large cynodont with a maximum known basal skull length of 290 mm; narrow and elongated skull with a concave outline in dorsal view; zygomatic arch with the jugal representing most of the dorsoventral depth and with a well-excavated external auditory meatus; heterodont postcanines including circular outlined anterior teeth, ovoid gomphodont teeth in the middle, and sectorial teeth posteriorly; relatively large subtemporal fossa; lack of a boss on the postorbital bar; maxillary gomphodont teeth longer labiolingually than mesiodistally, with a larger labial cusp and a smaller lingual cusp, connected by a transverse crest; usually three to five small mesiolingual and three to five small distolingual accessory cusps surrounding the perimeter of the crown in the unworn upper gomphodont teeth; lower gomphodont crowns usually longer labiolingually than mesiodistally, but in some instances the teeth may be circular in outline or longer mesiodistally than labiolingually; a large labial and a subequal lingual crown cusp are present, connected by a low transverse ridge, and surrounded by a variable number of small peripheral cusps; sectorial teeth multicusped, mesiodistally elongated, and with crowns dominated by a large, somewhat recurved labial cusp surrounded lingually by a well-developed cingulum, which generally supports from five to seven small cusps; and the conical and gomphodont tooth series both exhibit a size gradient, the most anterior tooth being considerably smaller than the most posterior tooth of each class. *Diademodon tetragonus* is characterized by the following postcranial features: axis lacking prezygapophyses; scapula with a straight anterior and a concave posterior margin in lateral view; interclavicle characterized by a short posterior crest and low and broad lateral and anterior crests in ventral view, and by a petaloid-shaped posterior process; manubrium concave dorsally and broader posteriorly than anteriorly; facet on the anterolateral corner of the manubrium not raised; first sternebra approximately as wide anteriorly as posteriorly; second sternebra with a facet for the third thoracic rib; relatively slender humerus with a very short nonexpanded portion of the diaphysis and the proximal portion not much expanded mediolaterally, contrasting with the very broad distal portion of the bone; deltopectoral crest short, less than half the total length of the humerus; laminar, medially expanded entepicondyle with a conspicuous pointy proximomedial projection; ilium with a relatively long ischial process and the anterior outline of the iliac blade presents two broad, gently concave sections separated by a convex region; ischium lacking a groove and a crest on its dorsal surface; and femur bearing a well-developed, crest-like lesser trochanter on its ventral surface reaching approximately the mid-length of the bone.

Note on the Diagnosis—*Diademodon tetragonus* has not been formally diagnosed, although several studies have dealt with its anatomy and taxonomy (e.g., Seeley, 1894; Watson, 1911, 1913; Brink, 1955, 1963, 1979; Fourie, 1963; Hopson, 1971; Osborn, 1974; Grine, 1977; Grine and Hahn, 1978; Grine et al., 1978, 1979; Gow and Grine, 1979; Botha and Chinsamy, 2000; Abdala et al., 2005; Martinelli et al., 2009; Liu and Olsen, 2010; Liu and Abdala, 2014). Despite our focus on the postcranium of *Diademodon tetragonus*, we include in the diagnosis cranial features of the species recognized by previous authors, mainly Martinelli et al. (2009) and Grine (1977).

Horizon and Locality—GSN R327 was collected at the western buttress of Etjo Mountain (central Namibia) in the nodule-bearing shale beds between two arenaceous horizons, from the lower levels of the Upper Omingonde Formation (Waterberg Basin).

DESCRIPTION

Vertebral Column

Cervical Vertebrae—The atlas-axis and the first three postaxial vertebrae (c3–c5) are articulated (Fig. 2). This series is very

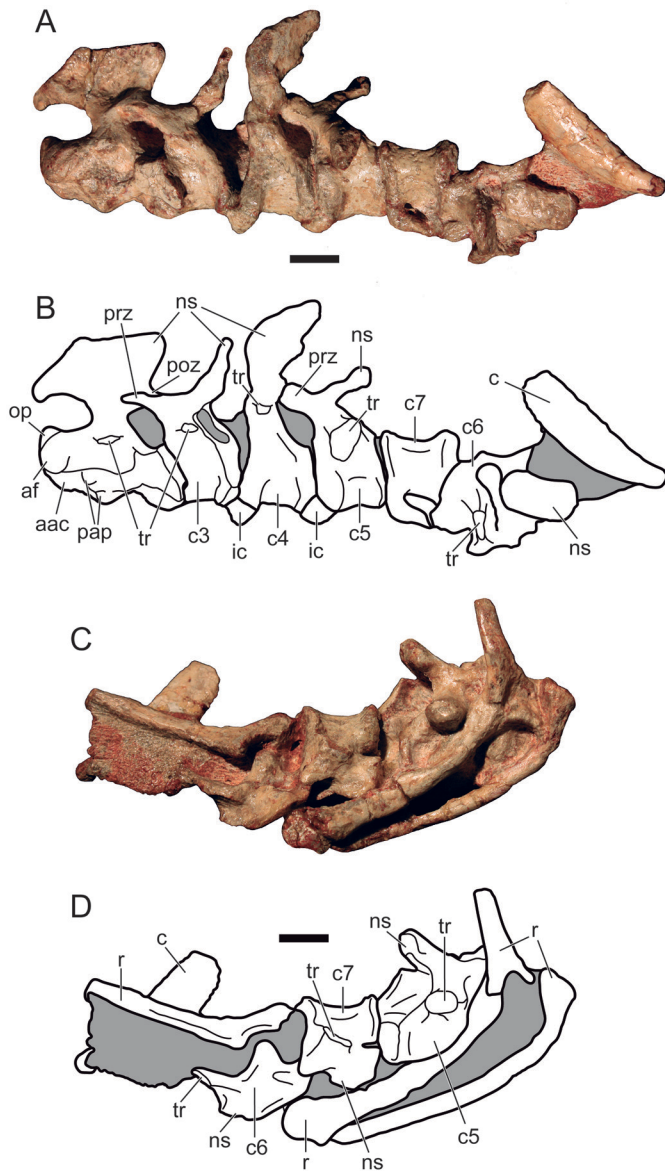


FIGURE 2. Cervical vertebrae of *Diademodon tetragonus* (GSN R327). **Abbreviations:** aac, atlas-axis centrum; af, atlas arch facet; c3–c7, vertebral centrum; op, odontoid process/dens; pap, parapophyses; poz, postzygapophyses; prz, prezygapophyses; ns, neural spine; tr, transverse process. Shaded areas indicate rock remains. Scale bars equal 10 mm.

close to two articulated vertebrae that are interpreted as the fourth and fifth postaxial cervical vertebrae (c6–c7), which are rotated upside-down and facing posteriorly (i.e., the c7 is in contact with the c5, not the c6). Posterior to these elements, there is an isolated fragmentary neural spine (Fig. 2).

The atlas-axis centrum is long and bears a poorly developed anterodorsally projecting odontoid process (Fig. 2A–B). Ventral to this process, a rugose, flat surface oriented anteroventrally represents the facet for the atlas intercentrum. In lateral view, the suture line between the atlas and axis centra is hinted at by an inflated region that separates anterior and posterior concave areas of the lateral surface of the centrum. Ventrally, this suture zone features well-developed parapophyses, which are connected by a high, blunt crest that marks the suture line (Fig. 2A–B). A mid-ventral keel is present in the posterior half of the vertebral body (posterior to the suture zone). The articular facet for the atlas

arch is large and slightly convex. It is surrounded by a groove anteriorly, ventrally, and posteriorly. The transverse processes are broken at their base, emerging from the neural arch close to the vertebral body. The axis neural spine is laminar and expanded anteroposteriorly, with a more pronounced anterior projection. Its anterior and dorsal margins are not preserved. The axial prezygapophyses were not developed. The postzygapophyses are articulated with the prezygapophyses of the c3 (Fig. 2A–B).

The vertebral body of c3 is spool-shaped, with a very depressed but almost flat central area and rimmed anterior and posterior margins in lateral aspect (Fig. 2A–B). The expanded anterior and posterior margins of the vertebral body represent the sites for attachment of the ribs. Small nutritive foramina are present on the lateral surface of the vertebral body. A mid-ventral keel is present. The neural arch is placed anteriorly. Broken at the base, the transverse process is close to the base of the neural arch and is inferred to have been oriented laterally and posteroventrally. The poorly preserved neural spine is posteriorly inclined. The prezygapophyses are at the end of long processes, extending forward to the anterior margin of the centrum (Fig. 2A–B). The postzygapophyses are not preserved.

Vertebra c4 only differs from c3 in the more dorsally placed base of the transverse process and in the better-developed anterior rimmed margin of the centrum (Fig. 2A–B). In c4, the postzygapophyses are placed at the level of the posterior margin of the neural arch and a central keel is present dorsally on the neural arch, anterior to the broken neural spine. These features are not preserved in c3.

The c5 is almost completely preserved except for the neural spine (Fig. 2A–B). The vertebral body is similar to that of c3 and c4 in general morphology. Unlike in c4, the anterior rimmed margin of the centrum is more inflated and extends more dorsally in lateral view, whereas the posterior margin of the vertebral body is much less expanded than in c4. The transverse processes are short, robust, and expanded distally. They are laterally and ventroposteriorly oriented. The neural arch is low and anteriorly placed. The prezygapophyses project anteriorly, exceeding the anterior margin of the vertebral body, as in c3. Only the base of the neural spine is preserved, but it can be ascertained that it was anteroposteriorly long and laterally compressed (Fig. 2A–B). As in c4, there is a central keel on the dorsal surface of the neural arch.

The intervertebral foramen between c4 and c5 is large but smaller than that between the axis and c3. The intercentra of c3, c4, and c5 are preserved in original position as small and triangular structures protruding ventrally with respect to the pleurocentra (Fig. 2A–B).

Only the incomplete neural arch of c6 is preserved (Fig. 2). The neural canal is small. The bases of the transverse processes suggest that they were oriented anterolaterally, probably an artifact, given the different orientation observed in c5 and c7. Similar to c4 and c5, there is a strong crest on the dorsal surface of the neural arch beginning at its anterior margin and continuing through what is preserved of the neural spine. The base of the neural spine hints that its orientation was similar to that of c5.

The vertebral centrum of c7 is spool-shaped as in the preceding postaxial vertebrae (Fig. 2). The anterior and posterior surfaces of the vertebral body are concave, making the centrum amphicoelous; however, it lacks the inflated anterior and posterior margins observed in c3–c5. The anterior and posterior margins of the vertebral body are crest-like in c7; thus, the facets for the capitulum of the anterior and posterior ribs are not conspicuous. A crest links the anterior margin of the vertebral body with the transverse process. The preserved base of the transverse process suggests that it was posterolaterally oriented (Fig. 2C–D). Ventrally, the vertebral body is flat to slightly convex and lacks a mid-ventral keel. Unlike the preceding cervicals, the neural arch is placed at the posterior portion of the centrum. The prezygapophyses only barely exceed the anterior margin of the vertebral body, and the articular facets are almost vertical (Fig. 2C–D). Similar to c4–c6, a

crest is also present on the dorsal surface of the neural arch and continues over the base of the neural spine.

Dorsal Vertebrae—A series of seven articulated but poorly preserved vertebrae are represented by incompletely preserved neural arches and are interpreted here as dorsal vertebrae. In order to make reference easy, we will refer to them as dx1 to dx7 from the anteriormost to the last one; however, it should be borne in mind that this does not imply that they represent the seven most anterior dorsal vertebrae.

The neural spine of the fragmentary neural arch of dx1 is laterally compressed; in lateral view, it is approximately rectangular, slightly widening anteroposteriorly towards the tip. It is oriented about 10° anterior to the vertical. In cross-section, the outline of the neural spine is triangular, with the anterior margin being broad and the posterior one acute.

Only the base of the transverse process remains of the dx2. Ventral to it, there is an indeterminate bone fragment that might belong to the same vertebra. The base of the transverse process is robust, compressed dorsoventrally (although not laminar in cross-section), and suggests a lateral and anterodorsal orientation.

The dx3 is the best-preserved vertebra of the series. The right side of the neural arch, transverse process, and part of the neural spine are relatively well preserved when compared with the left side of this element. Additionally, although deformed, the neural canal can also be observed. The neural spine is laterally compressed and is posterodorsally oriented, forming an angle with the horizontal of approximately 75°. The transverse process is placed anteriorly on the neural arch, being more dorsoventrally compressed and less robust than in dx2. It is oriented laterally and anterodorsally. The neural canal is reconstructed as low and wide.

A fragment of the neural spine, showing a similar orientation to that of dx3, and part of the neural arch is all that remains of dx4. Represented by a fragmentary neural arch, dx5 seems to be smaller than dx3 and dx7 and similar in size to dx4 and dx6. The transverse process is incompletely preserved and, oddly, seems to have been posteroventrally oriented. The base of the transverse process is relatively small and widens distally. The pre- and post-zygapophyseal processes are long and well separated from the neural spine, with the anterior one being larger than the posterior. The zygapophyseal facets cannot be observed. As in dx3 and dx4, the neural spine of dx5 is oriented posteriorly, with an angle close to 75° with respect to the horizontal.

Vertebra dx6 has a very laterally compressed neural spine that is similarly oriented to those of dx3–dx5. The transverse process in dx6 is deformed; it begins as a tubular, laterally narrow process directed posteroventrally and then widens and curves anteroventrally.

Vertebra dx7 is only represented by the neural spine and the very poorly preserved anterior portion of the neural arch. The neural spine is deformed and incomplete. It is tall and compressed laterally, rectangular in lateral aspect, triangular in cross-section, and oriented approximately 50° to the horizontal.

Scapula

The left scapula is completely preserved, although a few fractures are present and some sediment remains in the glenoid and coracoid contact areas (Fig. 3G–J). It is medially curved and shows a long and slender blade. In lateral view, the posterior margin of the scapular blade is concave, whereas the anterior one is approximately straight (Fig. 3G–H). In medial view, the scapula is flat in its

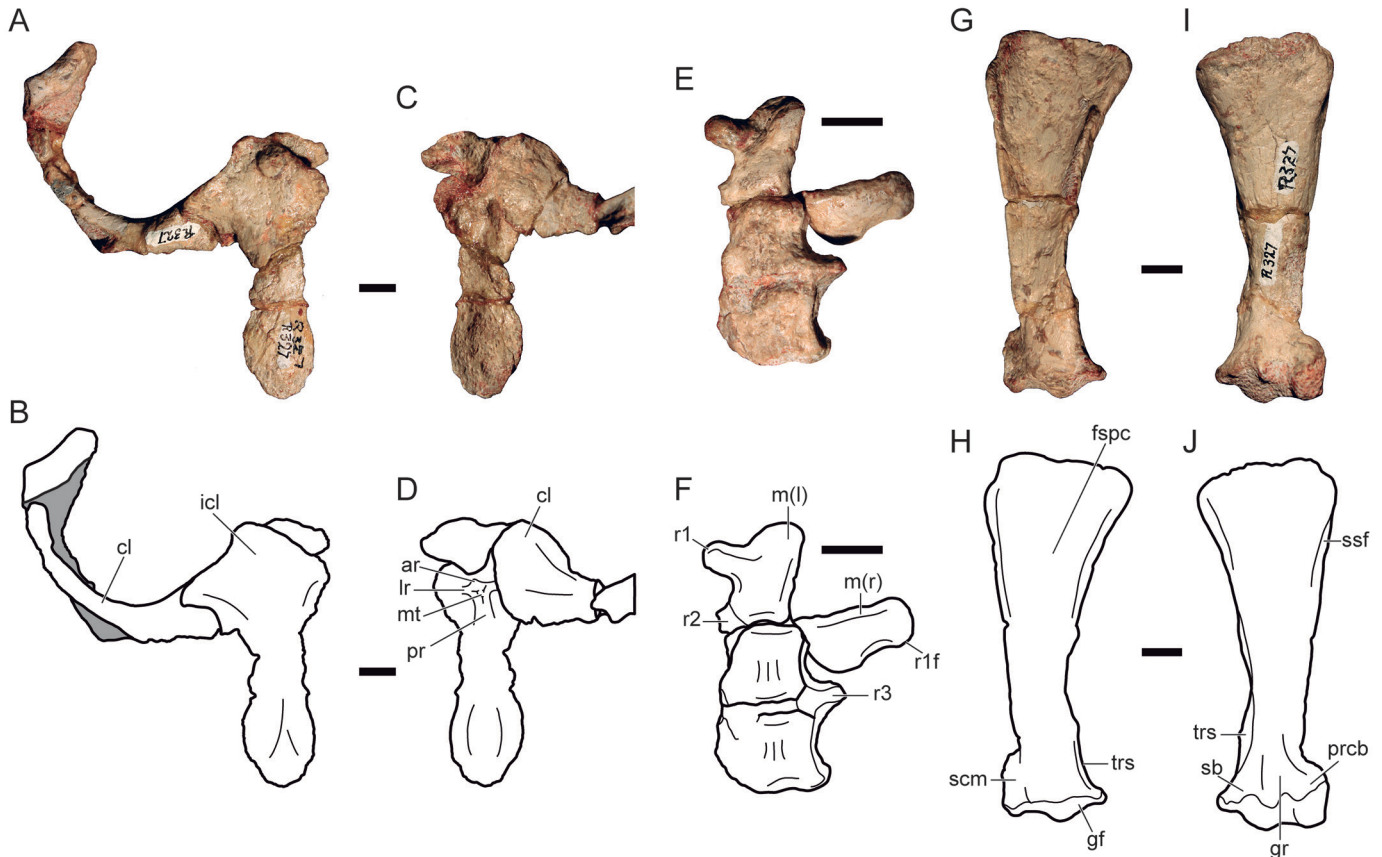


FIGURE 3. Shoulder girdle elements of *Diademodon tetragonus* (GSN R327). A–D, left clavicle and interclavicle in dorsal (A, B) and ventral (C, D) views. E–F, sternal elements in dorsal view. G–J, left scapula in lateral (G–H) and medial (I–J) views. **Abbreviations:** ar, anterior ridge; cl, clavicle; icl, interclavicle; fspc, suprascapoid (= infraspinatus) fossa; gf, glenoid facet; gr, groove; lr, lateral ridge; m(l), left manubrium; m(r), right manubrium; mt, median tuberosity; pr, posterior ridge; prcb, procoracoid buttress; r1–r3, thoracic ribs; r1f, facet for the first thoracic rib; sb, supraglenoid buttress; scm, insertion area for the m. suprascapoid; ssf, suprascapoid fossa; trs, groove for the origin for the scapular head of the m. triceps. Shaded areas indicate rock remains. Scale bars equal 10 mm.

dorsal-most portion and becomes progressively convex towards the neck and the glenoid region (Fig. 3I–J). The neck of the scapula is not very constricted compared with the scapular blade or the glenoid region. The acromion process is absent (Fig. 3G–J).

The dorsal margin is not perfectly preserved, although its general outline can be reconstructed as slightly convex, with the anterodorsal corner broadly curved and the posterodorsal one forming a more acute angle (between the dorsal and posterior margins). The posterodorsal corner of the scapular blade projects posteriorly in lateral view (Fig. 3G–J).

The supracoracoid (= infraspinus) fossa occupies the whole lateral surface of the scapula (Fig. 3G–H), with its anterior margin higher than the posterior one. This fossa becomes shallower ventrally, merging with the gently convex surface of the scapular neck. The anterior margin of the supracoracoid fossa is higher in the dorsal region of the scapula and continues ventrally through the neck into the articular facet for the procoracoid. The posterior margin reaches its highest point at mid-length of the scapular blade and becomes a low, blunt crest in the neck, ending in the glenoid facet. In posterior view, this highest area bears rugosities, representing the tubercle for the origin for the scapular head of the *m. triceps* as interpreted for *Cynognathus* (Seeley, 1895b: fig. 10; Jenkins, 1971). There is no evidence of a postscapular fossa on the posterior surface of the scapula. On the other hand, an incipient supraspinous fossa is present dorsally on the anterior surface of the scapular blade, limited medially by a triangular projection that corresponds to the anterodorsal corner of the scapula in medial view. Part of the supraspinous fossa can be observed in medial view (Fig. 3I–J).

The supraglenoid and procoracoid buttresses are separated by a broad groove that probably led to the procoracoid foramen (Fig. 3I–J). The procoracoid buttress is robust and triangular in anterior view. In lateral aspect, its surface is slightly concave, unlike the convex surfaces of the neck and glenoid region, and would have been the insertion area for the *m. supracoracoideus*. The procoracoid facet is ventrally oriented, whereas the coracoid facet is ventromedial. The glenoid is ventrolaterally oriented and is separated from the lateral surface of the scapula by a thin crest (Fig. 3G–H).

Clavicle

The left clavicle is preserved in articulation with the interclavicle, partially covered ventrally by a nonexpanded rib (Fig. 3A–D). The clavicle is strongly deformed, as is evident from the pronounced anterior curvature of the bone. The expanded medial region is plate-like, flat to slightly convex, and with a smooth surface (Fig. 3C–D). The clavicle becomes much thinner and tubular laterally.

Interclavicle

The interclavicle is almost complete and relatively well preserved, although there are some fractures and deformation and the bone margins are imperfectly preserved (Fig. 3A–D). It has a broad anterior portion and a long, laterally narrow posterior process. The rhomboidal anterior region has convex and concave areas dorsally, suggesting that it was affected by deformation (Fig. 3A–B). Ventrally, the anterior portion of the interclavicle bears broad, blunt anterior and lateral ridges. A short, low, and broad posterior ridge is also present. In the intersection of these ridges, a median tuberosity is present (Fig. 3C–D). The posterior ramus of the interclavicle has a spatulate outline. This posterior portion is flat, except in its widest region where it is convex dorsally and concave ventrally (Fig. 3C–D).

Sternum

Manubrium—The left half of the manubrium is preserved in articulation with two sternebrae posteriorly, although it is slightly medially displaced (Fig. 3E–F). The right half of the manubrium is not in its natural position. Thus, it is inferred that the two halves of the manubrium were not sutured but joined by soft tissue in this specimen. The manubrium was not fused with the first sternebra.

In dorsal view, the manubrium surface is slightly convex (Fig. 3E–F). The left half is triangular, with an acute anterior margin, probably due to breakage and some degree of deformation, whereas the right one is more or less rectangular, with a better-preserved, rounded anterior margin. The right half of the manubrium is thinner dorsoventrally and broader mediolaterally than the left half of this element. The right and left elements are more robust posteriorly than anteriorly (Fig. 3E–F).

In the right half of the manubrium, a blunt protuberance with an anterolaterally oriented facet for articulation with the first thoracic rib is present in the anterolateral corner (Fig. 3E–F). On the left manubrium, there is a tall, dorsally and anterolaterally directed projection approximately at mid-length of the bone that is interpreted as a fragment of the first thoracic rib. The position of this rib does not match the position of the corresponding facet present in the right half of the manubrium, suggesting that deformation might have occurred in the left portion of the manubrium and the associated first thoracic rib. The suture between the first rib and the left manubrium is not clearly observed. A posterolaterally directed process bears the facet for the second thoracic rib. The proximal end of the second thoracic rib is fused to the left half of the manubrium (Fig. 3E–F).

Sternebrae—Two sternebrae are preserved in articulation with the left half of the manubrium (Fig. 3E–F). They are dorsoventrally compressed and narrower than they are long in dorsal view. The first sternebra is well preserved. It is 1.3 cm long and 1.5 cm wide. The second sternebra is not so well preserved, especially the left lateral and posterior margins. It is slightly larger than the first sternebra (1.5 cm in anteroposterior length). Only the first sternebra can be observed in ventral view, showing a smoothly convex ventral surface. In dorsal view, the lateral margins of the sternebrae are concave and the central region is approximately flat. The dorsal surface of the first sternebra presents longitudinal crests and grooves on the central region that are absent from the second sternebra. In both elements, the suture line between the right and left halves is hinted at. The anterior margin of the first and second sternebrae is rimmed and presents rugosities. The anterior margin of the first sternebra is slightly convex, whereas it is straight in the second one. The posterior margin of the first sternebra is not rimmed and is straight. The posterior margin of the second sternebra is only partially preserved (Fig. 3E–F).

The sternebrae have anterolateral and posterolateral projections in their four corners (Fig. 3E–F). In the first sternebra, the left anterolateral projection is not preserved but the right one shows a dorsolaterally oriented facet, purportedly for the second thoracic rib. A posterolaterally oriented facet, to which the third thoracic rib is sutured, is present on the posterolateral corner of the first sternebra. This rib is also sutured to an anterolaterally oriented facet on the anterolateral projection of the second sternebra (Fig. 3E–F). A robust posterolateral projection is present in the second sternebra, but it is not well preserved.

Humerus

The right humerus is completely preserved, with only minor damage on the deltopectoral crest, but the distal portion appears to be deformed. The left humerus is represented only by its apparently nondeformed distal portion. The humeri are of the

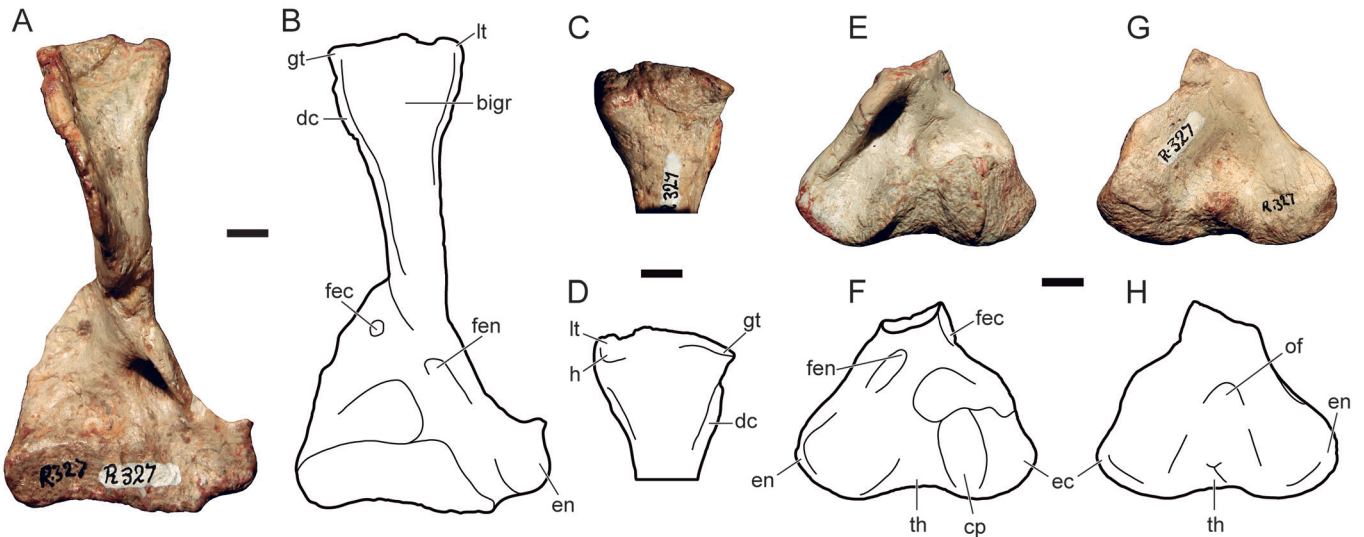


FIGURE 4. Humerus of *Diademodon tetragonus* (GSN R327). **A–D**, right humerus in ventral (**A–B**) and dorsal (**C–D**) views. **E–H**, left humerus in ventral (**E–F**) and dorsal (**G–H**) views. **Abbreviations:** **bigr**, bicipital groove; **cp**, capitulum; **dc**, deltopectoral crest; **ec**, ectepicondyle; **en**, entepicondyle; **fec**, foramen ectepicondylar; **fen**, foramen entepicondylar; **gt**, greater tuberosity; **h**, humeral head; **lt**, lesser tuberosity; **of**, olecranon fossa; **th**, humeral trochlea. Scale bars equal 10 mm.

same size, suggesting that they belong to the same individual (Fig. 4).

The humeral head is slightly expanded dorsolaterally, and is oriented proximally and laterally, with only a minor dorsal component. There is no clear limit between the humeral head and the dorsolateral surface of the bone (Fig. 4C–D).

The proximal surface of the humeral head is continuous with the greater and lesser tuberosities. This surface is rugose, suggesting the presence of a cartilaginous cap. The proximal margin between the humeral head and the greater tuberosity is poorly preserved, and the proximal-most portion of the deltopectoral crest is not preserved, precluding the recognition of the insertion area for the *m. supracoracoideus*. In proximal view, the deltopectoral crest–greater tuberosity forms an angle of approximately 90° with the axis of the humeral head–lesser tuberosity. The proximal surface of the humerus is very robust in the region of the lesser tuberosity, becoming progressively laminar towards the greater tuberosity. In dorsal aspect, there is a shallow and wide notch between the lesser tuberosity and the humeral head.

The lateral surface of the deltopectoral crest is flat distally and slightly concave proximally, where it is most robust (Fig. 4A–B). This concavity represents the fossa for the brachial musculature. On the other hand, the crests for the *m. latissimus dorsi* or the *m. teres minor* are not observed. The deltopectoral crest is thin distally but broadens slightly in its distal-most corner (terminal tuberosity of Jenkins, 1971), where it curves towards the diaphysis, representing the insertion area of the deltoid musculature.

In ventral view, the bicipital groove is strongly convex, its proximal third being deeper than the distal two-thirds, with a smooth, blunt, oblique crest separating both portions (Fig. 4A–B). In ventral aspect, the lesser tuberosity is very robust and has a rugose surface, suggesting that it was a site for strong muscular attachment. Distally, the lesser tuberosity continues as a low crest that disappears in the distal third of the bicipital groove, at the level of maximum height of the deltopectoral crest (Fig. 4A–B).

The diaphysis is short and robust, being broader dorsoventrally than mediolaterally (Fig. 4A–B). As judged from the left humerus, the humeral diaphysis cross-section has a triangular outline.

In ventral view, the laminar entepicondylar region of the right humerus is quadrangular and has a small proximomedial projection (Fig. 4A–B). In contrast to this, in the left humerus, the entepicondyle is robust; in ventral aspect, it is rounded and lacks a proximomedial projection, continuing without interruption into the bar medially limiting the entepicondylar foramen on the one side and into the distal surface of the humerus on the other (Fig. 4E–F). In medial view, the entepicondyle surface seems unfinished, suggesting that the medial flange of the entepicondyle might be broken, a fact that, together with some degree of dorsoventral compression on the distal portion of the right humerus, would provide an explanation for the differences in this region between the right and left humeri. The concave ventral surface of the entepicondyle continues into the entepicondylar foramen. This is separated from the humeral trochlea by a sharp and well-defined crest (Fig. 4A–B, E–F).

Ventrally, the humeral trochlea is slightly convex proximodistally and flat mediolaterally (Fig. 4E–F). It has a trapezoidal outline, expanding distally. Whereas the medial margin of the trochlea is crest-like and separated completely from the entepicondylar region by a groove, the lateral concave surface of the trochlea is continuous with the convex ectepicondylar region laterally. Dorsally, the trochlea continues as a pyramidal structure, limited laterally and medially by broad grooves continuous with the triangular olecranon fossa (Fig. 4G–H).

The capitulum is oval, with the long axis oriented proximodistally, and relatively narrow lateromedially when compared with the trochlea in ventral view (Fig. 4E–F). Lateral to the capitulum, there is a depressed rugose surface that continues into the lateral face of the humerus. The ectepicondyle is developed in this region as a small lateral projection, continuous with the distal surface of the humerus in ventral view (Fig. 4E–F). In ventral view, the lateral margin of the distal half of the humerus is concave in the left element and convex in the right one (Fig. 4A–B, E–F). This difference could be explained by the breakage of the very thin anterior margin of the left humerus in this area and by slight deformation of the right humerus. There is a well-defined oval concave depression proximal to the trochlea, the capitulum, and the ectepicondylar region in ventral view (Fig. 4A–B, G–H).

In the left humerus, the ectepicondylar foramen is approximately at the same level of the proximal region as the entepicondylar foramen in ventral view, whereas in the right humerus it is much proximally situated (Fig. 4A–B, E–F). On the other hand, in dorsal view, the ectepicondylar foramen is more proximally placed than the entepicondylar foramen in the left humerus. In the right humerus, there is a shallow groove on the lateral margin of the bone leading to the ectepicondylar foramen. In the left element, this groove is absent, probably due to breakage.

Radius

The almost complete left radius is known, although the epiphyses are not well preserved and there are fractures in the diaphysis (Fig. 5A–H). It is approximately straight, with slight curvatures in the proximal and distal regions. In medial and lateral views, the proximal end curves anteriorly and the distal one posteriorly. The

incompletely preserved facet for the ulna, recognized as an expanded area of the proximal epiphysis in posterior view, continues into a well-defined crest that broadens distally and might represent the radial tuberosity for the insertion of the biceps. This crest did not reach the mid-length of the radius, although breakage precludes observation of its distal end (Fig. 5C–D). Medial to this crest, there is the radial fossa, a shallow depression where the forearm flexors would have inserted (Fig. 5C–D, G–H). A very faint anterior lineation is present medially, beginning at the radial fossa and directed diagonally anterodistally (Fig. 5G–H). It continues as a low, blunt crest, reaching the distal region of the radius. The posterior lineation is also present in posterior to posterolateral view. It starts as a weak crest, and its distal end is not clearly identifiable (Fig. 5C–D). The distal tuberosity for the ulnar contact is directed posteriorly (Fig. 5C–H). The radial epiphyses are approximately triangular and are not strongly expanded (2 and 1.8 cm in medial view, proximally and distally) when compared with the diameter of the diaphysis (0.85 cm).

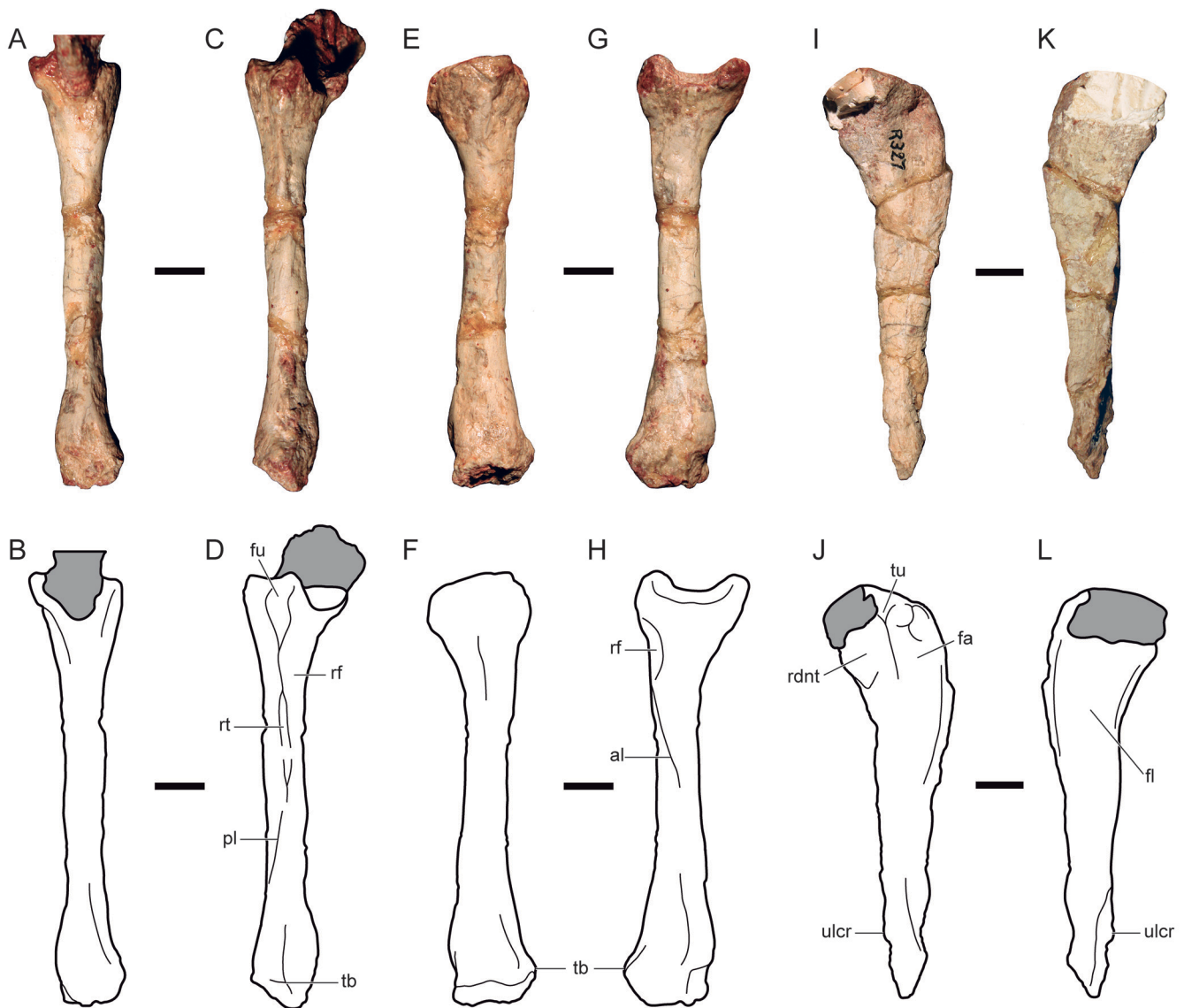


FIGURE 5. Radius and ulna of *Diademodon tetragonus* (GSN R327). A–H, left radius in anterior (A–B), posterior (C–D), lateral (E–F), and medial (G–H) views. I–L, left ulna in lateral (I–J) and medial (K–L) views. **Abbreviations:** al, anterior lineation; fa, fossa for adductor musculature; fl, origin area of the deep flexor musculature; fu, facet for articulation with the ulna; pl, posterior lineation; rdnt, radial notch; rf, radial fossa; rt, radial tuberosity; tb, distal tuberosity; tu, tuberosity; ulcr, ulnar crest. Shaded areas indicate rock remains. Scale bars equal 10 mm.

Ulna

The left ulna is partially preserved, with the distal portion missing and many cracks present. Plaster remains preclude complete observation of its proximal portion (Fig. 5I–L). The ulna is almost straight in medial view and slender, compressed mediolaterally, relatively unexpanded anteroposteriorly, and long proximodistally. In anterior view, it is slightly curved medially, with the medial margin concave and the lateral one straight. The sigmoid facet cannot be properly observed but is interpreted to have been oriented anteroproximally, with its long axis approximately aligned with that of the ulna in anterior view. Only the distal section of a very thin and, judging from the preserved portion, relatively low ulnar crest is present (Fig. 5I–L). In posterior aspect, the proximal area of the ulna is expanded mediolaterally and bears striations, representing the area for the connection of a nonossified olecranon process. A well-defined crest runs obliquely from the proximal expansion for the olecranon, ending proximal to the distal tubercle over the medial margin of the posterior surface of the ulna. The distal tubercle is broken but seems to have been well developed.

Medially, there are two relatively depressed areas separated by a faint convexity. These depressions are interpreted as the origin area of the deep flexor musculature (Fig. 5K–L). In lateral aspect, the proximal region of the ulna bears two fossae separated by a triangular tuberosity projecting laterally (Fig. 5I–J). The anterior fossa corresponds to the triangular, almost flat, and anterolaterally oriented radial notch. The posterior fossa is longer proximodistally and more concave than the radial notch. It is interpreted to have held adductor musculature. This posterior fossa becomes shallower distally, disappearing at approximately one-quarter of the length of the ulna, and includes, in its proximal area, two approximately circular depressions, the most anterior of which is relatively shallow and developed on the tuberosity that separates this fossa from the radial notch.

Ilium

The right ilium is partially preserved (Fig. 6A–D). The iliac blade is incomplete posteriorly and dorsally, and the dorsal portion of the anterior margin of the bone is missing. The iliac blade is slightly concave laterally and convex medially. Laterally, the blade bears very subtle radial striations. Medially, there is no evidence of articular facets for the sacral ribs. The anterior outline of the iliac blade presents two broad, gently concave sections separated by a convex region (Fig. 6A–B). The ventral margin of the posterior portion of the iliac blade is interpreted as oblique to the horizontal (Fig. 6A–B). The acetabular region of the ilium is very robust. The process for the ischium is a well-developed, posteroventrally oriented projection separated by a broad, but not very deep acetabular notch from the robust supra-acetabular buttress (Fig. 6A–B). The process for the pubis contact is broken off, but it can be reconstructed as forming a higher angle to the horizontal than the process for the ischium. The acetabulum is large when compared with the size of the femoral head.

Ischium

The head and neck region of two right ischia have been recovered. One of them is preserved in its natural position in contact with the right ilium (Fig. 6A–D) and is slightly smaller than the other one. The articular facets for the ilium and pubis cannot be readily observed in either of the specimens due to their mode of preservation and matrix remains. The acetabular facet of the ischium is anterodorsally and laterally oriented. It is concave and approximately oval. A rectangular ventral projection of the acetabular facet is interpreted to have contacted the pubis. The lateral surface of the preserved portion of the ischia is convex, whereas the medial surface is flat or slightly concave. The ventral

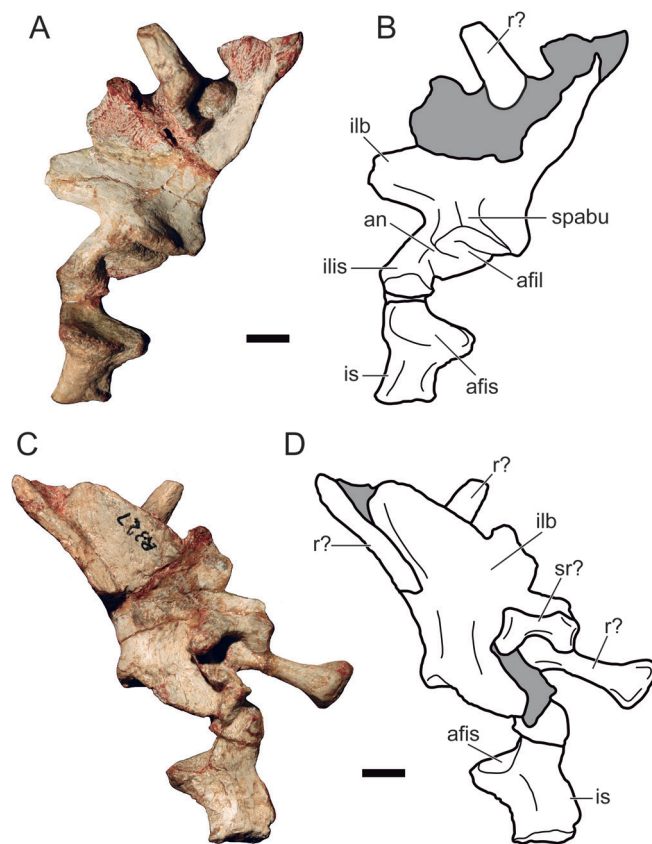


FIGURE 6. Pelvic girdle elements of *Diademodon tetragonus* (GSN R327). A–D, right articulated ilium and ischium in lateral (A–B) and medial (C–D) views. **Abbreviations:** *afil*, acetabular facet of the ilium; *afis*, acetabular facet of the ischium; *an*, acetabular notch; *ilb*, iliac blade; *ilis*, iliac process for the ischium; *is*, ischium; *r?*, rib; *spabu*, supra-acetabular buttress; *sr?*, sacral rib. Shaded areas indicate rock remains. Scale bars equal 10 mm.

margin of the ischial neck is concave, representing the postero-dorsal margin of the obturator foramen (Fig. 6A–D). In cross-section, the neck of the ischium is triangular, with a robust dorsal region and a laminar ventral one. Dorsally, the medial edge of the bone is higher than the lateral one.

Femur

There are three femora preserved. Two of them, only known by the proximal portion, are a right and a left element of very similar size and morphology, whereas the third femur recovered is a left element that preserves the diaphysis and the lesser trochanter but lacks the distal portion of the bone, the femoral head, and most of the greater trochanter. This latter femur represents a slightly larger individual than the other two elements (Fig. 7).

The proximal portion is slightly curved dorsally with respect to the diaphysis in medial view (Fig. 7E–F). The articular surface of the femoral head is rough or ‘unfinished’ and placed proximally and medially. The femoral head is connected to the greater trochanter through a crest that is not perfectly preserved proximally. The greater trochanter is clearly more robust than this crest (Fig. 7G–H). The lesser trochanter is a tall, thin, and sharp crest, well separated from the femoral head and ventrally directed (Fig. 7A–B, I–J). Medially, the lesser trochanter edge is convex, high

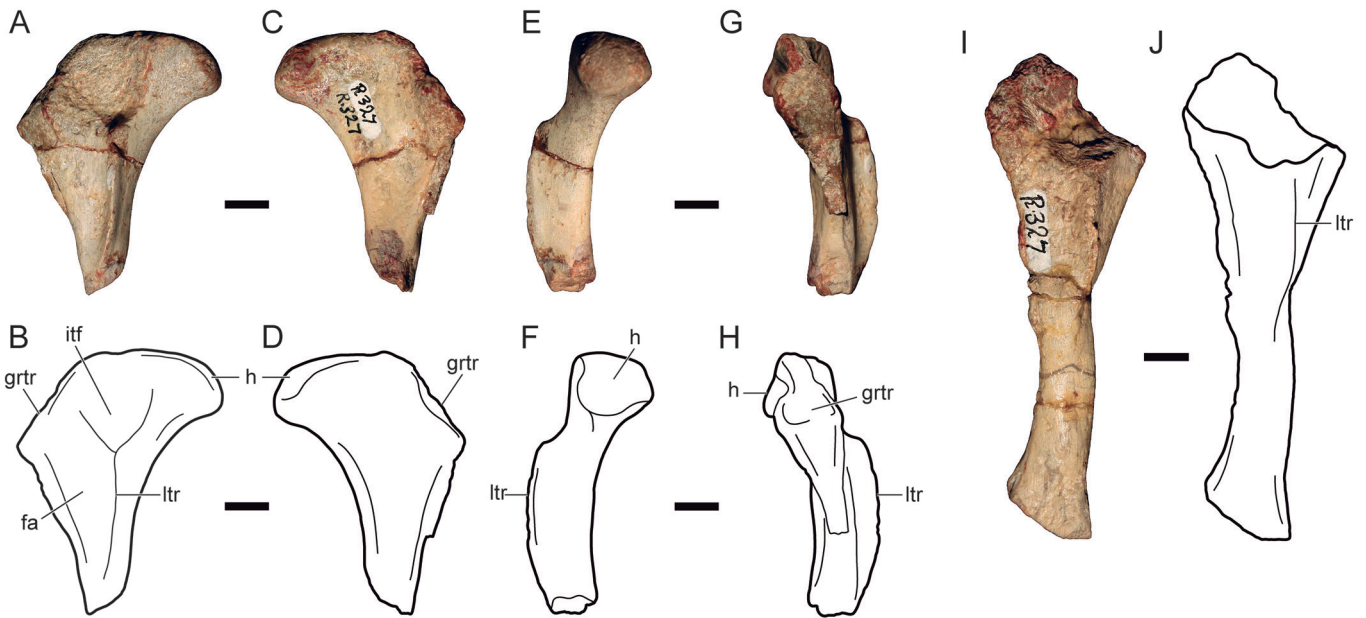


FIGURE 7. Femur of *Diademodon tetragonus* (GSN R327). **A–H**, left femur in ventral (**A–B**), dorsal (**C–D**), medial (**E–F**), and lateral (**G–H**) views. **I–J**, left femur in ventral view. **Abbreviations:** **fa**, fossa for adductor musculature; **grtr**, greater trochanter; **h**, femoral head; **itf**, intertrochanteric fossa; **ltr**, lesser trochanter. Scale bars equal 10 mm.

proximally and low distally (Fig. 7E–F). In ventral view, its distal third is slightly laterally curved, whereas proximally it continues as a low and blunt crest that contacts the proximal margin of the femur. This crest constitutes the medial edge of the intertrochanteric fossa, limited laterally by the greater trochanter. Distal to the intertrochanteric fossa, there is a concave, elongated, shallower area that represents the fossa for the adductor musculature (Fig. 7A–B). The dorsal surface of the femur, except for the proximal rim between the femoral head and the greater trochanter, is flat to slightly concave (Fig. 7C–D).

Fibula

The right fibula has been recovered. The bone is fractured, and its proximal region is incomplete. The distal portion is not preserved (Fig. 8). The fibula is an anteroposteriorly compressed element, curved in anterior/posterior view (the medial margin is concave and the lateral one is convex). The fibular tubercle is partially preserved (Fig. 8A–B, G–H). Medially, a short crest (medial ridge of Jenkins, 1971) is present on the proximal fifth of the fibula (Fig. 8A–E). There is an oval depression between the fibular tubercle and the medial ridge. Aligned with the medial ridge and separated by a small gap, a second crest (anteromedial ridge of Jenkins, 1971) is present (Fig. 8E–F). This latter crest curves anteriorly, reaching the anterior margin of the fibula in medial aspect, at the level of the distal region of the fibular tubercle. The anteromedial ridge does not continue distally as a distinct crest. A faint posteromedial ridge is present in the mid-portion of the fibular shaft (Fig. 8E–F). This ridge runs distally and posteriorly becoming the posterior edge of the bone. A posterolateral ridge is observed laterally on the proximal third of the fibula (Fig. 8G–H). This crest is relatively short, not exceeding the midportion of the fibular tubercle. The lateral crest is interpreted to be present but is not clearly observed due to preservational problems.

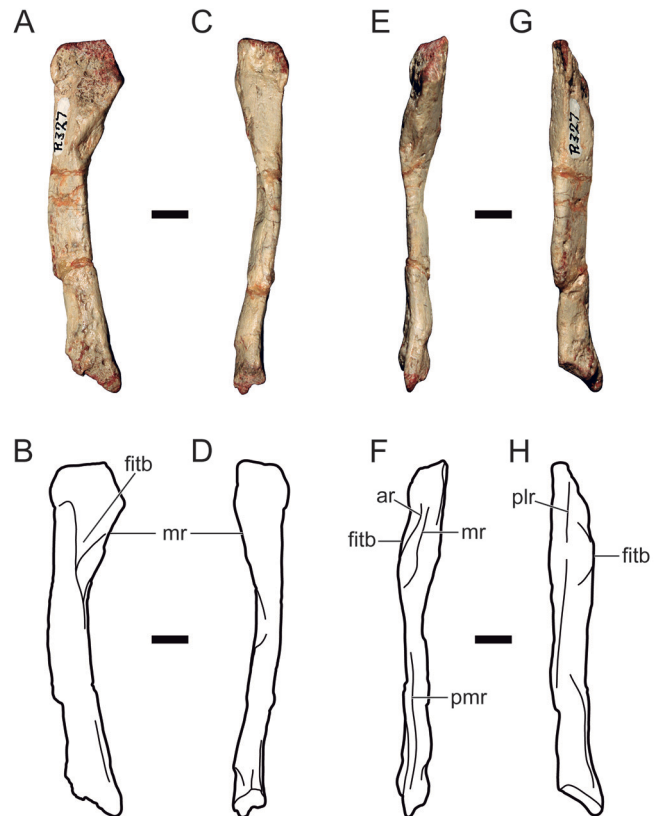


FIGURE 8. Fibula of *Diademodon tetragonus* (GSN R327). **A–H**, right fibula in anterior (**A–B**), posterior (**C–D**), medial (**E–F**), and lateral (**G–H**) views. **Abbreviations:** **ar**, anteromedial ridge; **fitb**, fibular tubercle; **mr**, medial ridge; **plr**, posterolateral ridge; **pmr**, posteromedial ridge. Scale bars equal 10 mm.

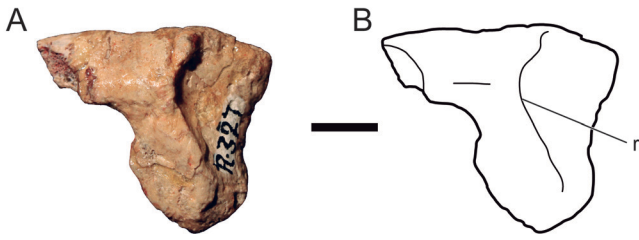


FIGURE 9. Lumbar rib of *Diademodon tetragonus* (GSN R327). **A–B**, right lumbar rib in dorsal view. **Abbreviation:** r, dorsal ridge. Scale bar equals 10 mm.

Lumbar Rib

An expanded right lumbar rib is almost entirely preserved (Fig. 9A–B). The anterior margin is evenly compressed. A dorsal ridge is present, and is only slightly laterally reflected on its anterior half. The dorsal ridge separates the robust medial portion from a laminar lateral region that contacted the preceding lumbar rib. Other articular facets, such as those described by Jenkins (1971), are not recognized. Ventrally, the surface of the expanded portion of the rib is slightly concave. The neck of the lumbar rib is approximately triangular in cross-section, with the anterior edge thicker than the posterior one.

COMPARISONS

We performed comparisons of the postcranium of *Diademodon tetragonus* with cynodonts, especially with other cynognathians, in order to analyze the morphological variation in the clade. The sternal elements of *Diademodon tetragonus* recognized only in GSN R327 were compared with those of tritylodontids, up to now the only non-mammaliaform cynodonts in which these bones have been reported. We considered the previously published information, mainly Seeley (1895a, 1895b), Watson (1917), Huene (1935–1942), Brink (1955), Crompton (1955), Kühne (1956), Bonaparte (1963, 1966), Jenkins (1970, 1971), Kemp (1980), Sun and Li (1985), Abdala (1999), Sues and Jenkins (2006), Oliveira et al. (2007), Kammerer et al. (2008), Liu et al. (2008, 2017), Liu and Powell (2009), and Pavanatto et al. (2016). Additionally, we personally analyzed specimens of *?Cynognathus/?Diademodon* (BPI 1675), *Diademodon* (USNM V23352), *Kayentatherium wellsi* (MCZ 8812), and *Massetognathus pascuali* (MCZ 3691, MCZ 3801, MCZ 3812, MCZ 3813, MCZ 4018, PVL 3688, PVL 4442, PVL 4613, PVL 5444, PVL S/N).

Vertebral Column

Cervical Vertebrae—Jenkins (1971) reported a collection of *?Cynognathus/?Diademodon* (BPI 1675) disarticulated postcranial skeletons containing isolated and incomplete atlas-axis elements. According to this author, there are no morphological differences among the few specimens recovered to distinguish the two genera. Additionally, according to Jenkins (1971), the atlas-axis complex of *?Cynognathus/?Diademodon* (BPI 1675) is very similar to those of *Thrinaxodon* and *Galesaurus*. Following this opinion, we will include comparisons of GSN R327 with the elements of *Thrinaxodon* and *Galesaurus* as figured and described by Jenkins (1971), considering them as a proxy for the morphology of specimen BPI 1675. Similar to the condition in GSN R327, the atlas and axis centra are fused in *Diademodon* (GSN R202 and GSN R205; Brink, 1955), *?Cynognathus/?Diademodon* (BPI 1675), *Gomphognathus* (= *Diademodon*) *kannemeyeri* (AM 458; Broom, 1903), *Cynognathus* (NHMUK 2571), *Massetognathus pascuali* (MCZ 3691), and *Menadon* (Kammerer et al., 2008). In *Exaeretodon argentinus*, the

odontoid process is not completely ossified together with the axial body (Bonaparte, 1963), and in *E. riograndensis* these elements are unfused (Oliveira et al., 2007). The facet for the atlas intercentrum is relatively broad laterally in GSN R327 as in *Diademodon* (GSN R202 and GSN R205) and *Massetognathus pascuali* (MCZ 3691), whereas it is relatively narrow in *Thrinaxodon* (Jenkins, 1971: fig. 2). Similar to what is observed in GSN R327, the parapophyses are separated from the articular facet for the atlas arch by a well-developed groove in *Diademodon* (GSN R202 and GSN R205) and *Cynognathus* (NHMUK 2571). In *M. pascuali* (MCZ 3691), the groove between the parapophyses and the facet for the atlas arch is shallow and not well defined. The parapophyses appear to be absent in the axis of *Thrinaxodon* and *Galesaurus* (Jenkins, 1971:figs. 2–3) and also in *Menadon*. The transverse processes of GSN R327 emerge from the neural arch of the axis in a relatively more anterior position when compared with *Diademodon* (GSN R202 and GSN R205), *Cynognathus* (NHMUK 2571), *M. pascuali* (MCZ 3691), and *Menadon*. Unlike in GSN R327 and *Menadon*, in which the axial prezygapophyses are not developed, these structures seem to be well developed in *Thrinaxodon* and *Galesaurus* (Jenkins, 1971:figs. 2–3). In *M. pascuali* (MCZ 3691), although not completely preserved in the specimens available, the prezygapophyses were interpreted to be vestigial (Jenkins, 1970). Brink (1955) did not mention the presence of axial prezygapophyses in *Diademodon* (GSN R202 and GSN R205) but represented them in a line drawing (Brink, 1955:fig. 5). The neural spine in the axis of *M. pascuali* (MCZ 3691) is notably less anteriorly projected than in the other taxa analyzed, including GSN R327, *Diademodon* (GSN R202 and GSN R205), *Cynognathus* (NHMUK 2571), *Menadon*, *Thrinaxodon*, and *Galesaurus*. A strong mid-ventral keel is present in the axis of *Cynognathus* (NHMUK 2571), a shared trait with GSN R327.

Brink (1955) did not provide a description of the postaxial cervical vertebrae of *Diademodon*. He only presented a drawing of the last four cervical vertebrae in lateral view of the purported *Diademodon* specimen GSN R227, precluding proper comparisons with GSN R327. GSN R327 shares with GSN R227, *Exaeretodon riograndensis*, *Massetognathus pascuali* (MCZ 3691), and *Menadon* the general shape of the postaxial cervical vertebrae centrum, including the amphicoelous condition and the rimmed anterior and posterior margins. The general morphology of the postaxial cervical centra of *Cynognathus* (NHMUK 2571) is similar to that of GSN R327 but with the anterior and posterior margins not as swollen. Unlike in GSN R327, a mid-ventral keel and a crest anterior to the neural spine are not present in any of the postaxial cervical vertebrae of *M. pascuali* (MCZ 3691) or in the first postaxial cervical vertebra of *E. riograndensis*. As in GSN R327, a mid-ventral keel is present in the postaxial cervical vertebrae of *Cynognathus* (NHMUK 2571) and *E. riograndensis*. The presence of a crest anterior to the neural spine is shared by GSN R327, *Exaeretodon argentinus*, and *Cynognathus* (NHMUK 2571). Unlike GSN R327, *Menadon* has well-developed parapophyses below the transverse processes. Similar to GSN R327, there are postaxial cervical intercentra in *Cynognathus* (NHMUK 2571), *E. riograndensis*, and the purported *Diademodon* specimen GSN R227; however, in *E. riograndensis*, *Menadon*, and GSN R227, the intercentra are not sutured to the pleurocentra, as in GSN R327 and *Cynognathus* (NHMUK 2571). *M. pascuali* (MCZ 3691) and *E. argentinus* lack postaxial cervical intercentra.

Dorsal Vertebrae—The fragmentary preservation of the dorsal vertebrae of GSN R327 precludes significant comparisons with other taxa.

Scapula

The outline of the scapular blade of GSN R327 differs from that of other cynognathians. In particular, there is much variation regarding the shape of the anterior and posterior

margins of the blade in lateral view. The anterior margin of the scapular blade is markedly convex in lateral view in *?Cynognathus/?Diademodon* specimens of Jenkins (1971) (e.g., NMB C2711), not straight as in GSN R327. Similar to the condition in *?Cynognathus/?Diademodon* specimens (sensu Jenkins, 1971), the anterior margin of the scapula of *Andescynodon* and *Menadon* is strongly convex in lateral view, giving the scapular blade a bowed outline. In GSN R224, a specimen that Brink (1955) assigned to *Diademodon laticeps*, and in *Pascualgnathus* (Bonaparte, 1966), the anterior and posterior margins of the scapular blade are concave. This condition differs from that in GSN R327 in which only the posterior margin is concave. The outline of the scapula of *Cynognathus* (NHMUK 2571) and *Luangwa drysdalli* (see Kemp, 1980) presents a concave anterior margin, whereas the posterior margin shows two concavities separated by a projected median region, thus differing from the straight anterior margin and the evenly concave posterior margin of GSN R327. Moreover, according to the illustrations of Kemp (1980), the scapula of *Luangwa drysdalli* is slightly anteriorly bowed as seen in lateral view, differing from the posteriorly curved scapula of GSN R327. In *Exaeretodon argentinus* (see Bonaparte, 1963:fig. 15) and the articulated *Massetognathus pascuali* individual in specimen MCZ 3691 illustrated by Jenkins (1970), the anterior margin of the scapula is concave and the posterior one straight, thus the scapula bows anteriorly, whereas the opposite is observed in GSN R327. Unlike that of GSN R327, the scapular blade of *Boreogomphodon* is rectangular, with the long axis of the blade inclined posteriorly (Liu et al., 2017). In *Traversodon*, the posterior margin of the scapula is concave in lateral view as in GSN R327; the posterior margin is broken, precluding comparisons (Huene, 1935–1942:pl. 17.12; Liu et al., 2017:fig. 10O–P).

Specimen GSN R327 shares the absence of an acromion process with *Andescynodon* (Liu and Powell, 2009) and *?Cynognathus/?Diademodon* specimens analyzed by Jenkins (1971). On the other hand, this structure is well developed in *Boreogomphodon*, *Cynognathus* (NHMUK 2571), *Exaeretodon argentinus*, *Luangwa drysdalli*, *Menadon*, *Pascualgnathus*, and *Traversodon* (Seeley, 1895b; Huene, 1935–1942; Bonaparte, 1963, 1966; Kemp, 1980; Kammerer et al., 2008; Liu et al., 2017). A relatively small but well-defined acromion process is present in *Diademodon* specimen GSN R224 (*D. laticeps* sensu Brink, 1955). According to Jenkins (1970), the acromion process is either not preserved or lacking in *Massetognathus pascuali*, similar to the condition in GSN R327. However, in *M. pascuali* specimen PVL 4613, a completely preserved, very well-developed acromion process is present (Liu et al., 2017:fig. 10K–L). In other *M. pascuali* specimens (MCZ 4249, PVL 5444, and PVL 5687), the acromion process is also present but it is incompletely preserved.

Specimen GSN R327 also differs from the *?Cynognathus/?Diademodon* specimens described by Jenkins (1971) in the absence of a groove ventral to the supracoracoid fossa (e.g., NMB C2711), a dorsal groove for the origin of the teres major in the posterior surface of the scapula, and a depression for the teres minor in the lateral surface of the scapular blade of large cynodonts (e.g., BPI 1675).

Compared with the scapula of GSN R327, the scapula of *Cynognathus* (NHMUK 2571) and GSN R224 (Seeley, 1895b; Brink, 1955; Liu et al., 2017:fig. 10C–D) is more rectangular and the neck is not as constricted. A well-developed process for the trigenus muscle (according to Brink, 1955) is present in *Cynognathus* (NHMUK 2571), GSN R224, and *Traversodon* (Huene, 1935–1942), whereas it is absent in GSN R327. This process seems to correspond in position with the area interpreted by other authors (e.g., Jenkins, 1971) to be the origin for the scapular head of the m. triceps as interpreted for *Cynognathus* (Seeley,

1895b:fig. 10; Jenkins, 1971). In medial view, in GSN R224, the supraspinous fossa is very well defined and even broader than in *Andescynodon* (see below) when compared with the poorly developed supraspinous fossa of GSN R327. Unlike what is observed in GSN R327, the dorsal portion of the supraspinous fossa is observable in lateral view in *Cynognathus* (NHMUK 2571). In *Traversodon*, the well-developed supraspinous fossa faces laterally, extending from the dorsal margin of the scapula to the acromion process, and the supracoracoid fossa is very shallow, differing notably from the general pattern observed in other cynognathians (Huene, 1935–1942).

The scapula of GSN R327 is more slender and relatively higher than those of *Luangwa drysdalli* and *Boreogomphodon*. In lateral view, in *Luangwa drysdalli* and *Boreogomphodon*, the dorsal margin of the scapular blade is as broad anteroposteriorly as the ventral region of the scapula, whereas in GSN R327 the dorsal margin is broader (Kemp, 1980:fig. 10A; Liu et al., 2017:fig. 10). In medial view, the areas for the origin of the m. supraspinatus and the m. subcoracoscapularis complex are more extended anteriorly and posteriorly and the central flat to convex portion is relatively narrower in *Luangwa drysdalli* when compared with GSN R327 (Kemp, 1980).

Compared with that of GSN R327, in *Pascualgnathus* the glenoid faces much more laterally (Bonaparte, 1966; Liu et al., 2017:fig. 10E). Additionally, unlike GSN R327, *Pascualgnathus* lacks evidence for the m. triceps insertion and bears a dorsoventrally broad acromion process (Bonaparte, 1966).

Contrary to what is observed in GSN R327, in *Exaeretodon argentinus* the posterodorsal corner of the scapula is rounded and the anterodorsal corner is projected anteriorly (Bonaparte, 1963; Liu et al., 2017:fig. 10H).

In *Andescynodon* and *Menadon*, both the anterodorsal and posterodorsal corners of the scapular blade form right angles, whereas in GSN R327 the anterodorsal corner is more gently curved (Kammerer et al., 2008; Liu and Powell, 2009). Although incompletely preserved dorsally, the supraspinous fossa is broader and better defined in *Andescynodon* than in GSN R327 as observed in medial view (Liu and Powell, 2009). The infraspinatus fossa is deeper in *Andescynodon* than in GSN R327 (Liu and Powell, 2009), a condition also shared by *Massetognathus pascuali*, although in this species the fossa is anteroposteriorly narrower than in GSN R327.

Clavicle

Only subtle differences and variations in the relative proportions of the clavicle are recognized between GSN R327 and other cynognathians. The clavicle of GSN R327 is more slender than those of *?Cynognathus/?Diademodon* (NMB C2700; Jenkins, 1971:fig. 24) and *Exaeretodon argentinus* (see Bonaparte, 1963). The clavicle of GSN R327 is relatively shorter than that of *E. argentinus* and longer than those of *Andescynodon* and *Pascualgnathus* (Bonaparte, 1963, 1966; Liu and Powell, 2009). When compared with *Andescynodon* and *Pascualgnathus*, the clavicle of GSN R327 is thinner, whereas it is more robust relative to that of *Massetognathus pascuali* (PVL 4613). When compared with GSN R327, *M. pascuali* (PVL 461) has a slightly more expanded medial region of the clavicle and *Pascualgnathus* presents a slightly more expanded lateral region (Bonaparte, 1966). In GSN R327, the medial portion of the clavicle is more expanded and the lateral portion not as expanded as in *Andescynodon* (Liu and Powell, 2009). The medial region of the clavicle of GSN R327 lacks the striations of *?Cynognathus/?Diademodon* in ventral view (NMB C2700; Jenkins, 1971:fig. 24B).

Interclavicle

The unambiguous *Diademodon* specimen SAM-PK-K5266 (Gow and Grine, 1979) shares with GSN R327 the petaloid-shaped posterior process of the interclavicle, the short posterior

crest, and the low and broad lateral and anterior crests in ventral view. However, some differences are also recognized. The posterior end of the interclavicle is more acuminate in SAM-PK-K5266 than in GSN R327. Ventrally, there are longitudinal striations on the posterior portion of the interclavicle of SAM-PK-K5266, which are absent in GSN R327.

In the partially preserved interclavicle of the cynognathian DMSW R 435 (Jenkins, 1971), the anterior portion of the posterior ramus is not as constricted as in GSN R327. In DMSW R 435, the posterior ridge is long, continuing posteriorly along the ventral surface of the posterior ramus of the interclavicle, thus differing from the very short posterior ridge of GSN R327.

In specimen NHMUK 3772a (a 'cynognathid' sensu Watson, 1917, and probably *Diademodon* according to Abdala, 1999), the interclavicle lacks the long lateral processes of the anterior region that are present in GSN R327. Additionally, specimen NHMUK 3772a has very protruding anterior process, differing from GSN R327. Ventrally, unlike in GSN R327, in specimen NHMUK 3772a the anterior and posterior ridges are thin and are separated from each other, and the median tuberosity and the lateral ridges are absent.

In GSN R327, the posterior process of the interclavicle is long and petaloid-shaped, whereas in *Exaeretodon argentinus* it is short and trapezoidal (Bonaparte, 1963). Unlike GSN R327, *E. argentinus* lacks lateral ridges and shows a thin ridge that runs from the anterior to the posterior margin of the interclavicle in ventral view. In dorsal view, the interclavicle of *E. argentinus* has anteriorly convex areas corresponding to the ventral placement of the clavicles and a depressed axial region, thus differing from the condition in GSN R327.

The outline of the interclavicle of GSN R327 is approximately similar to that of *Massetognathus pascuali* specimen PVL 4613; however, in PVL 4613, the anterior projection of the anterior margin of the interclavicle is less prominent and narrower than in GSN R327. In dorsal view, longitudinal striations are present on the posterior process of the interclavicle of *M. pascuali* (PVL 4613) but absent in GSN R327. Unlike in GSN R327, a long posterior ridge is present ventrally along the posterior ramus of the interclavicle in *M. pascuali* (PVL 4613) and has also been identified by Jenkins (1970) in other specimens.

Unlike in GSN R327, in *Boreogomphodon* the anterior portion of the interclavicle is not expanded laterally and the posterior portion is rectangular (Liu et al., 2017). In addition, the ridges on the ventral surface of the anterior region of the interclavicle are comparatively less developed in *Boreogomphodon* than in GSN R327.

Sternum

Manubrium—Comparisons of the manubrium are restricted to tritylodontids, the only nonmammaliaform cynodonts in which this structure is represented. Similar to *Kayentatherium* and *Bienotheroides*, the right and left manubria are preserved disarticulated, suggesting that these bones were not sutured to each other, differing from the condition observed in *Oligokyphus* (Kühne, 1956; Sun and Li, 1985; Sues and Jenkins, 2006).

Whereas the manubrium of GSN R327 has a convex dorsal surface, in tritylodontids this bone is distinctly concave dorsally. Similar to *Bienotheroides*, the anterior margin of the manubrium of GSN R327 is not bilobed, as in *Kayentatherium* and *Oligokyphus*. On the other hand, in *Bienotheroides*, the manubrium is laterally broader anteriorly than posteriorly, whereas the opposite is observed in GSN R327. *Bienotheroides* shares with *Oligokyphus* an anteriorly broad manubrium. In *Kayentatherium*, the anterior portion of the bone is almost as broad as the posterior one. As in GSN R327, the posterior margin of the manubrium in dorsal aspect is concave in *Bienotheroides* and *Kayentatherium*, unlike the straight posterior margin in *Oligokyphus*. In GSN

R327, the bone is thicker anteriorly than posteriorly as in *Oligokyphus* but contrary to the condition in *Kayentatherium*. The facet on the anterolateral corner of the manubrium is not raised in GSN R327 as it is in *Kayentatherium* and *Oligokyphus*. In *Bienotheroides*, this facet is more anteriorly oriented than in other tritylodontids and GSN R327. In *Oligokyphus*, there are two facets in this area, one for the coracoid and a more posterior one for the first thoracic rib. In GSN R327, *Bienotheroides*, and *Kayentatherium*, there is only one anterolateral facet. In GSN R327, the facet on the posterolateral corner of the manubrium is comparatively large, similar to *Kayentatherium*, whereas it is proportionally smaller in *Bienotheroides* and *Oligokyphus*. In GSN R327, this facet is at the end of a relatively robust posterolateral projection that is not raised dorsally as in *Kayentatherium*. The posterolateral projection is similarly oriented in GSN R327 and *Bienotheroides*. In *Oligokyphus*, there is no posterolateral projection and the facet for the second thoracic rib is on the rim of the manubrium.

Sternebrae—Similar to what is observed in GSN R327, the sternebrae of tritylodontids (*Kayentatherium* and *Oligokyphus*; Kühne, 1956; Sues and Jenkins, 2006) were not sutured to the manubrium. In GSN R327 and *Oligokyphus*, the first and second sternebrae were sutured to each other, whereas this is not the case in *Kayentatherium*. The first and second sternebrae of *Oligokyphus* are different from those of *Kayentatherium* and GSN R327 in general shape, being proportionally anteroposteriorly long and laterally narrow. In *Kayentatherium*, these bones are wider than long, whereas the opposite is observed in GSN R327. Contrary to our interpretation of GSN R327, the first sternebra of *Kayentatherium* and *Oligokyphus* does not articulate with the third thoracic rib. Compared with *Kayentatherium* and *Oligokyphus*, the first sternebra of GSN R327 is laterally expanded anteriorly. As in GSN R327, there is a suture line between the right and left halves of the first sternebrae in *Kayentatherium*. On the other hand, *Kayentatherium* lacks the longitudinal crest and grooves present on the dorsal surface of the first sternebra of GSN R327. Unlike in GSN R327, the anterior and posterior margins of the first and second sternebrae of *Kayentatherium* are not well preserved and appear 'unfinished,' suggesting the presence of a cartilaginous cap. In *Kayentatherium*, the articular facets for the third thoracic rib are not readily recognizable as in GSN R327.

Humerus

The humerus of *Diademodon* specimen SAM-PK-K5266 has not been illustrated or described properly (Gow and Grine, 1979), precluding comparisons with GSN R327.

Seeley (1895a) presented the humerus of *Microgomphodon eumerus* (NHMUK 3581), a specimen inferred to be a tiny *Diademodon* according to Brink (1955:31). Incomplete preparation and the single drawing provided by Seeley (1895a) preclude proper comparisons between NHMUK 3581 and GSN R327. The proximal half of the humerus NHMUK 3581 seems broader than that of GSN R327 in ventral view. The rotation of the proximal half of the humerus NHMUK 3581 with respect to the distal one appears to be different from GSN R327, that is, whereas the proximal half is observed in ventral view, the distal half is presented as if it was the medial view in GSN R327; although a fracture is present between these two sections in NHMUK 3581, Seeley (1895a) did not attribute the rotation to deformation.

Seeley (1895a) also described and illustrated the humerus NHMUK R2579 assigned to *Gomphognathus* (= *Diademodon*; Brink, 1955; Watson and Romer, 1956). Unlike in GSN R327, in Seeley's specimen the deltopectoral crest is longer than half the total length of the humerus. In ventral aspect, the crest that is continuous with the lesser tuberosity is longer and more robust in NHMUK R2579 than in GSN R327. Several differences are

also recognized in the distal portion of the bone between these specimens. Unlike that in GSN R327, the capitulum in NHMUK R2579 is not so far from the lateral margin of the bone; the entepicondyle is rounded and relatively robust, only poorly projected proximally; and the ectepicondyle is comparatively better defined and more expanded proximodistally. Additionally, there are muscle insertion marks on the ent- and ectepicondyles that are not observed in GSN R327.

Watson (1917) described a complete humerus that he assigned to a 'Cynognathid' (NHMUK 3772a). Later, Abdala (1999) concluded that this element may in fact belong to *Diademodon*. Unlike that of *Diademodon* specimen GSN R327, the humerus of NHMUK 3772a is more robust, the proximal portion is broader mediolaterally, and the distal portion of the humerus is shorter proximodistally and not as broad mediolaterally. The deltopectoral crest is more extended laterally in NHMUK 3772a than in GSN R327, allowing for a broader bicipital groove. In NHMUK 3772a, the deltopectoral crest is longer proximodistally than in GSN R327. Additionally, the entepicondyle in NHMUK 3772a is not as projected medially, is shorter proximodistally, and bears a faint proximomedial projection when compared with GSN R327. The capitulum in NHMUK 3772a is more developed than that in GSN R327 and reaches the lateral margin of the bone.

The humerus of specimen GSN R327 is similar to that of *Cynognathus*?/*Diademodon* specimen NMB C2693 studied by Jenkins (1971). Although there are some differences, most of them seem to be related to muscle development and insertion. The humeral head in NMB C2693 is more inclined dorsally than in GSN R327. The dorsal lip of the humeral head, separating the head from the dorsal surface of the humerus of NMB C2693, is absent in GSN R327. The crests on the dorsal surface of the humerus of NMB C2693 for the m. latissimus dorsi or the m. teres minor are not identified in GSN R327, which also lacks the striations and rugosities for the m. pectoralis insertion that were described in NMB C2693. The bicipital groove is not divided by a crest in NMB C2693, as it is in the humerus of GSN R327.

The distal half of the right humerus of GSN R327 is mediolaterally broader than in NMB C2693, a fact that could be due to deformation of the Namibian specimen. In ventral aspect, in the right humerus of GSN R327, the triangular depression proximal to the capitulum and trochlea and the broad groove between the trochlea and the entepicondyle are only poorly defined when compared with NMB C2693. In the right humerus of GSN R327, the laminar entepicondyle is more expanded medially and shorter proximodistally than in NMB C2693 in ventral view. Additionally, the small projection of the entepicondyle points proximally in NMB C2693 but proximomedially in the right humerus of GSN R327. In the left humerus of GSN R327, the entepicondyle is robust and rounded, without a flange-like structure medially, as observed in the right humerus of GSN R327 and in NMB C2693. The medial surface of the entepicondyle of the GSN R327 left humerus is 'unfinished,' suggesting that the medial flange of the entepicondyle is broken. Ventrally, the triangular depression proximal to the trochlea and the capitulum is deeper in the right and left humeri of GSN R327 than in NMB C2693. Proximal to this depression, the lateral margin of the humerus is straight in NMB C2693 in ventral view, whereas it is concave in the left humerus of GSN R327 and expands laterally, becoming convex in the right humerus of GSN R327. The difference in the mentioned margin between NMB C2693 and the right humerus of GSN R327 could be explained by deformation in GSN R327. The difference from the left humerus of GSN R327 could be due to the breakage of the very thin lateral margin of the humerus in this area. In the left humerus of GSN R327, the ectepicondylar foramen is just proximal to the level of the proximal region of the entepicondylar foramen in ventral view, whereas in the GSN R327 right humerus and NMB C2693 it is

relatively more proximally situated. On the other hand, in dorsal view, the ectepicondylar foramen is more proximally placed than the proximal end of the entepicondylar foramen in the left humerus, opposite to the condition in NMB C2693. In the right humerus of GSN R327, there is a shallow groove on the lateral margin of the bone leading to the ectepicondylar foramen as in NMB C2693. In the left element, this groove is absent.

The humerus of SAM-PK-K4002, found in association with lower jaws of *Diademodon*, is partially preserved and can only be observed in dorsal and lateral views. As in GSN R327, the distal portion is much more expanded than the proximal portion and the deltopectoral crest extends distally approximately until the middle of the diaphysis (Abdala, 1999:table 4). The distal portion of SAM-PK-K4002 resembles strongly the isolated distal portion of GSN R327 (Fig. 4G–H), with no evidence of the proximomedial projection on the entepicondyle described in the complete humerus GSN R327 (Fig. 4A–B), a fact that can be attributed to postmortem damage.

The humerus of *Cynognathus* (PVL 3859; Abdala, 1999) is more slender than that of GSN R327, showing a long diaphysis and a relatively much less mediolaterally expanded distal portion. The deltopectoral crest in PVL 3859 is not as expanded as, and is proportionally longer than, in GSN R327. In dorsal aspect, in PVL 3859, the olecranon fossa is deep and the trochlea is only poorly developed in comparison with GSN R327.

When compared with that of GSN R327, the humerus of *Exaeretodon argentinus* is stout and robust and has a more dorsally oriented humeral head (Bonaparte, 1963). The deltopectoral crest in *E. argentinus* is longer than half the total length of the bone, whereas it is shorter in GSN R327. In GSN R327, the terminal tuberosity of the deltopectoral crest is not so pronounced as in *E. argentinus*. In *E. argentinus*, the insertion area for the m. pectoralis is well developed ventrally on the distal half of the deltopectoral crest, whereas this muscle insertion area is not readily recognizable in GSN R327. Additionally, the deltopectoral crest is more flaring in *E. argentinus* than in GSN R327. Unlike in GSN R327, the bicipital groove is not divided by a crest in *E. argentinus*. In dorsal aspect, the trochlea is subspherical in *E. argentinus*, differing from the condition in GSN R327. The small proximal projection of the entepicondyle of GSN R327 is absent in *E. argentinus*, and the entepicondyle is relatively higher proximodistally in *E. argentinus* than in GSN R327.

When compared with the condition in GSN R327, the humeral head is more projected dorsolaterally in the fully prepared humerus of *Massetognathus pascuali* specimen MCZ 3691. A slightly different condition is observed in *Massetognathus ochagaviae* (see Pavanatto et al., 2016), in which the humeral head is projected dorsally to a greater degree than in GSN R327. The diaphysis of the humerus of *M. pascuali* (MCZ 3691) is better defined and relatively longer when compared with GSN R327, whereas in *M. ochagaviae* it is more robust than in both GSN R327 and MCZ 3691. In *M. pascuali* (MCZ 3691) and *M. ochagaviae*, the deltopectoral crest is more laminar (not so robust) than in GSN R327. The terminal tuberosity of the deltopectoral crest is absent in the humerus of *M. pascuali* and *M. ochagaviae*, whereas it is present in GSN R327. Unlike in GSN R327 and *M. pascuali* (MCZ 3691), in *M. ochagaviae* the deltopectoral crest is longer than half the length of the humerus. The crest continuing distally from the lesser tuberosity is longer and very robust in *M. pascuali* (MCZ 3691) when compared with the one in GSN R327. The distal portion of the humerus of *M. pascuali* (MCZ 3691) is only poorly expanded mediolaterally when compared with GSN R327 in dorsal/ventral view. In *M. pascuali* (MCZ 3691), the entepicondyle is less projected medially when compared with GSN R327. The entepicondyle of *M. ochagaviae* has a not so well defined proximal projection as in GSN R327 or in *M. pascuali* (MCZ 3691). The flange continuous with the ectepicondyle in dorsal view is more flaring in *M. ochagaviae* than in

GSN R327 or *M. pascuali* (MCZ 3691). The olecranon fossa is more extended proximodistally in *M. pascuali* (MCZ 3691) than in GSN R327.

The humeral head in *Andescynodon* has a more dorsal component than in GSN R327 (Liu and Powell, 2009). Unlike in GSN R327, the deltopectoral crest is longer than half the length of the humerus in *Andescynodon*. In *Andescynodon*, the entepicondyle is more projecting than in GSN R327 but lacks the proximal projection of the latter. In ventral view, the capitulum is well separated from the anterior margin of the bone in *Andescynodon*, whereas there is almost no separation in GSN R327. The bicipital groove is deeper and more extended in GSN R327 than in *Andescynodon*; however, this could be due to postmortem deformation of the known specimens.

Similar to that of GSN R327, the humerus of *Pascualgnathus* is slender, with a relatively short deltopectoral crest (Bonaparte, 1966; Liu et al., 2017:fig 11B). The humerus of *Pascualgnathus*, as figured by Liu et al. (2017), differs from that of GSN R327 in presenting a longer nonexpanded portion of the diaphysis, a not so mediolaterally expanded distal region, a medially expanded area for the m. triceps insertion (as interpreted by Bonaparte, 1966), an entepicondyle that is not laminar and with a more robust proximomedial projection, poorly developed ulnar condyle and capitulum ventrally, and a large and deep depression in the distal region of the humerus as seen in ventral view. Additionally, the proximal portion of the bone seems to be rotated approximately 90° with respect to the distal portion in *Pascualgnathus* (Liu et al., 2017:fig 11B). On the other hand, the drawings by Bonaparte (1966) show the humerus of *Pascualgnathus* with a relatively expanded distal portion, a laminar entepicondyle, and torsion between the proximal and distal portions of the humerus, similar to what is observed in GSN R327. Additionally, according to Bonaparte's (1966) interpretation, the capitulum and ulnar condyle of *Pascualgnathus* are similar-sized, ovoid, longer mediolaterally than proximodistally, and separated by a narrow trochlear region in ventral view.

The humerus of *Luangwa drysdalli* differs from that of GSN R327 in the longer deltopectoral crest, the less expanded distal portion, the more robust entepicondyle with a less developed proximomedial projection, the capitulum closer to the lateral margin of the humerus, the larger trochlea and olecranon fossa in dorsal view, and the similar-sized, rounded capitulum and ulnar condyle separated by a narrow trochlea in ventral aspect (Kemp, 1980; Liu et al., 2017:fig 11C). In the humerus of *Boreogomphodon*, the nonexpanded portion of the diaphysis is longer than that in GSN R327. Unlike in GSN R327, the entepicondyle in the humerus of *Boreogomphodon* is not laminar but robust; it is not expanded medially and lacks a proximomedial projection. In *Boreogomphodon*, the ectepicondylar foramen is closed, whereas it is open in GSN R327. In ventral view, in *Boreogomphodon*, the ulnar condyle and the capitulum are bulbous, have a circular outline, and are separated by a narrow trochlea, differing from what is observed in GSN R327.

Only a reconstruction of the humerus of *Cricodon* has been published (see Crompton, 1955). When compared with GSN R327, in *Cricodon* the entepicondyle lacks the proximal projection and is not so medially expanded. In ventral aspect, the greater tuberosity is more expanded proximally in *Cricodon* than in GSN R327.

Radius

The radius of GSN R327 is more robust than that of *?Cynognathus/?Diademodon* BPI 1695. In anterior view, the lateral margin of the radius is concave in *?Cynognathus/?Diademodon* BPI 1695, whereas it is straight in GSN R327. In *?Cynognathus/?Diademodon* BPI 1695, the radial crest is sigmoid and becomes thinner distally, unlike the straight radial

crest of GSN R327 that broadens distally. Compared with that of GSN R327, the radial fossa is deeper and more distally positioned in *?Cynognathus/?Diademodon* BPI 1695. In *?Cynognathus/?Diademodon* BPI 1695, the anterior lineation is clearly observed, unlike the very faint crest present in GSN R327. Similarly, the posterior lineation is better defined in *?Cynognathus/?Diademodon* BPI 1695, especially distally and in lateral view.

In *Exaeretodon argentinus* and *Exaeretodon riograndensis*, the radius is notably more robust than in GSN R327. Unlike that of GSN R327, the radius of *E. argentinus* has a better-defined and larger radial fossa and bears tubercles and rugosities probably associated with muscle insertion. Unlike in GSN R327, the radial crest runs oblique medially in *E. argentinus*, not straight as in GSN R327.

Unlike that of GSN R327, the radius of *Pascualgnathus* is sigmoid in lateral/medial aspect and has an expanded proximal region that tapers distally towards a very reduced distal end in lateral/medial view. According to Bonaparte (1966), the radius of *Pascualgnathus* lacks a radial fossa, a radial crest, and the anterior and posterior lineations. As Bonaparte (1966) already suggested, the radius of *Pascualgnathus* is very similar to an ulna, leading us to wonder if the bone published as the radius is not in fact a poorly preserved ulna.

The radius of GSN R327 is more robust than specimen MCZ 3691 of *Massetognathus pascuali* (the one described by Jenkins, 1970) and has less expanded proximal and distal regions than *Massetognathus ochagaviae* (see Pavanatto et al., 2016). The radius of GSN R327 is slightly less sigmoid than those of *M. ochagaviae* and *M. pascuali* (MCZ 3691). Unlike in GSN R327, in *M. pascuali* (MCZ 3691) the radial crest reaches the mid-length of the radius as a well-defined sharp crest. Medially, a crest interpreted as the anterior lineation is better defined in *M. pascuali* (MCZ 3691) than in GSN R327. In posterior view, there is a shallow concavity between this crest and the tuberosity for the ulnar contact in *M. pascuali* (MCZ 3691), absent in GSN R327. Additionally, a very pronounced crest is present on the lateral margin of the radius in the distal third of the radius of *M. pascuali* (MCZ 3691), but not in GSN R327.

Ulna

The ulna of *?Cynognathus/?Diademodon* BPI 1675 differs in several aspects from that of GSN R327. In *?Cynognathus/?Diademodon* BPI 1675, the ulna is not straight but sigmoid, more robust, and comparatively broader anteroposteriorly and mediolaterally when compared with GSN R327. In anterior view, opposite to the condition in GSN R327, the ulna of *?Cynognathus/?Diademodon* BPI 1675 is slightly curved laterally instead of medially, with a concave lateral margin and an approximately straight medial margin. In posterior view, the area for the insertion of an unossified olecranon process is more robust in *?Cynognathus/?Diademodon* BPI 1675 than in GSN R327. In *?Cynognathus/?Diademodon* BPI 1675, the fossa for the extensor musculature is more conspicuous than in GSN R327. Additionally, the two small circular depressions recognized in lateral view in the proximal region of GSN R327 are absent in *?Cynognathus/?Diademodon* BPI 1675.

The ulna of *Exaeretodon argentinus* and *Exaeretodon riograndensis* is notably robust, with an ossified olecranon process, differing from that of GSN R327. In anterior view, in *E. argentinus*, the ulna is not medially curved as in GSN R327, but straight and the sigmoid facet is oblique, not aligned with the long axis of the bone as in GSN R327 (Bonaparte, 1963; Liu et al., 2017:fig. 13E).

The ulna of *Pascualgnathus* is more sigmoid than that of GSN R327 in lateral/medial view (Bonaparte, 1966; Liu et al., 2017:fig. 13C). In anterior aspect, the distal portion of the ulna is more expanded lateromedially in GSN R327 than in

Pascualgnathus. Although not present in the holotype of *Pascualgnathus*, Bonaparte (1966) reported the presence of an ossified olecranon process in the ulna of MLP 65-IV-18-2, differing from GSN R327 in which this process is absent. The anterior fossa on the distal half of the lateral face of the ulna of *Pascualgnathus* is not present in GSN R327.

The isolated ulna of *Massetognathus pascuali* specimen MCZ 3691 (the one studied by Jenkins, 1970) is more sigmoid than that of GSN R327 in lateral/medial view. In medial view, the crest on the posterior margin is better developed and the fossae on the medial surface of the ulna are more conspicuous in *M. pascuali* (MCZ 3691) than in GSN R327. In lateral view, the crest on the posterior margin limiting the extensor fossa is better developed in *M. pascuali* (MCZ 3691) than in GSN R327. The two small fossae in the proximal region of the extensor fossa in GSN R327 are absent in *M. pascuali* (MCZ 3691).

In lateral aspect, the proximal portion of the ulna of *Andescynodon* is relatively more expanded anteroposteriorly and more strongly bowed anteriorly than in GSN R327 (Liu and Powell, 2009).

Ilium

Brink (1955) described the ilium of *Diademodon* as having a semicircular and rounded anterior margin, a condition that differs from that in specimen GSN R327.

The ilium of GSN R327 differs from those of *?Cynognathus/?Diademodon* (BPI 1695) and *?Aleodon/?Scalenodon* (NHMUK 8) specimens figured by Jenkins (1971:figs. 44 and 46, respectively). Unlike in GSN R327, the anterior margin of the iliac blade is rounded in lateral view in *?Cynognathus/?Diademodon* (BPI 1695) and *?Aleodon/?Scalenodon* (NHMUK 8; see Jenkins, 1971; Liu et al., 2017:fig. 14A), whereas the anterior outline of the iliac blade of GSN R327 presents two broad, gently concave portions separated by a convex one. Unlike in other analyzed taxa, the anterior margin of the ilium of GSN R327 is very similar to what is known of *Microgomphodon eumerus* (NHMUK 3581, reinterpreted as *Diademodon* by Brink, 1955) as figured by Seeley (1895a:pl. 1). If oriented in life position, the anterior portion of the iliac blade of *Cynognathus* (NHMUK 2571), *?Cynognathus/?Diademodon* (BPI 1695), and *?Aleodon/?Scalenodon* (NHMUK 8) appears as less dorsally projected than in GSN R327. The ischial process in *Cynognathus* (NHMUK 2571), *?Cynognathus/?Diademodon* (BPI 1695), and *?Aleodon/?Scalenodon* (NHMUK 8) is relatively short when compared with that in GSN R327. The thickening of the blade anterodorsal to the acetabulum and the associated vertical crest and two resultant shallow fossae described by Jenkins (1971) for *?Cynognathus/?Diademodon* (BPI 1695) and *?Aleodon/?Scalenodon* (NHMUK 8) are not present in GSN R327.

The orientation of the ilium of *Exaeretodon argentinus* has been interpreted to be very different from that of GSN R327 (see Bonaparte, 1963:fig. 9; Liu et al., 2017:fig. 14G), with the supra-acetabular buttress anteriorly placed and the process for the ischium in a posterior position. If oriented similarly as in GSN R327, the long axis of the iliac blade of *E. argentinus* would be almost dorsoventrally oriented, differing from the usual approximately anteroposterior orientation present in other cynodonts. In *E. riograndensis*, the iliac blade is anteroposteriorly oriented, similar to the orientation in *E. argentinus* as interpreted by Bonaparte (1963). Unlike in GSN R327, in *E. argentinus* there is not a flange anterior to the supra-acetabular buttress and the anterior margin of the iliac blade in lateral view is straight to slightly concave. In *E. argentinus*, the lateral surface of the iliac blade is strongly convex and bears a strong ridge in its middle portion, whereas in GSN R327 it is only slightly concave and lacks a ridge. What is preserved of the postacetabular portion of

the iliac blade in lateral view in GSN R327 is higher than that in *E. argentinus*.

The ilium of *Pascualgnathus* has a relatively long, well-developed neck, absent in GSN R327. If similarly oriented (based on the acetabular region), the preacetabular portion of the iliac blade is more anteriorly and less dorsally projected in *Pascualgnathus* than in GSN R327. In lateral view, the anterior margin of the iliac blade of *Pascualgnathus* is evenly convex, unlike that of GSN R327. According to the illustrations provided by Bonaparte (1966:fig. 9) and Liu et al. (2017:fig. 14B), and unlike in GSN R327, a well-developed supra-acetabular buttress and a flange anterior to it are absent in *Pascualgnathus*.

In *Massetognathus pascuali*, the neck and acetabular portion of the ilium is more slender than in GSN R327, in which the neck is not so constricted. The anteroventral margin of the iliac blade in lateral view is straight to slightly convex in *M. pascuali*, whereas it bears two concave regions and one convex region in GSN R327. The process for the ischium is short in *M. pascuali*, unlike in GSN R327. If similarly oriented, GSN R327 and both species of *Massetognathus* differ in the orientation of the pre- and post-acetabular portions, which show a much more marked dorsal component in GSN R327. The ilium of *Massetognathus ochagaviae* (UNIPAMPA 0625; Pavanatto et al., 2016) has a less slender neck and a shorter, more dorsally projected preacetabular portion of the iliac blade when compared with specimens of *Massetognathus pascuali*.

In *Luangwa drysdalli*, the process for the ischium is very short, unlike in GSN R327. If similarly oriented, unlike in GSN R327, the postacetabular portion of the iliac blade would point posteroventrally in *L. drysdalli*. In *L. drysdalli*, the supra-acetabular buttress is less robust and the neck is more constricted than in GSN R327. The anterior margin of the iliac blade of *L. drysdalli* is concave in the ventral region and convex in the dorsal one, differing from what is observed in GSN R327, in which the dorsal region is also concave and is separated from the ventral concave portion by a convexity (Kemp, 1980; Liu et al., 2017:fig. 14D).

Unlike in GSN R327, in *Andescynodon* and *Menadon* the anterior margin of the iliac blade is straight in the ventral half and convex in the dorsal one. In *Andescynodon*, the supra-acetabular buttress is poorly developed and the ischial process very short, unlike in GSN R327. A conspicuous ischial process is absent in *Menadon*. The neck of the ilium is more constricted in *Andescynodon* than in GSN R327. If similarly oriented (i.e., the neck approximately vertical), the preacetabular portion of the iliac blade is more pronouncedly projected anteriorly than dorsally in *Andescynodon* and *Menadon*, whereas the opposite is observed in GSN R327.

The ilium of GSN R327 is very similar to that of *Belesodon magnificus* (sensu Huene, 1935–1942:pl. 14). Compared with GSN R327, *Belesodon* has a shorter process for the ischium and, if similarly oriented, the preacetabular portion of the iliac blade more anteriorly oriented.

Ischium

Contrary to GSN R 327 and *Boreogomphodon* (Liu et al., 2017), a groove and a crest on the dorsal region of the ischium are present in the specimens analyzed by Jenkins (1971), *?Cynognathus/?Diademodon* (NMB C2702), *Cynognathus* (NHMUK 2571), *?Aleodon/?Scalenodon* (NHMUK 8), *Andescynodon* (Liu and Powell, 2009), *Exaeretodon argentinus* (see Bonaparte, 1963), *Massetognathus pascuali* (PVL 5444, PVL 3688, PVL 4613, MCZ 4018), *Menadon* (Kammerer et al., 2008), and *Pascualgnathus* (Bonaparte, 1966).

In *Exaeretodon argentinus* (see Bonaparte, 1963), *Luangwa drysdalli* (see Kemp, 1980), *Massetognathus* (PVL 5444, MCZ 4018), *Menadon* (Kammerer et al., 2008), and *Pascualgnathus* (Bonaparte, 1966), there is a well-developed crest or projection

anteriorly limiting the acetabular facet of the ischium that is absent in GSN R327.

The ischium is relatively thicker (mediolaterally) in the neck region in *Massetognathus pascuali* (PVL 5444, PVL 3688, PVL 4613, MCZ 4018) and *Luangwa drysdalli* when compared with GSN R327.

Femur

The proximal region of the femora of GSN R327 is very similar to that of *?Cynognathus/?Diademodon* (NMB C2694; Jenkins, 1971), but the greater trochanter is relatively less robust and the diaphysis expands distally more gradually in *?Cynognathus/?Diademodon* NMB C2694 when compared with GSN R327. In *?Cynognathus/?Diademodon* NMB C2694 and in *Cynognathus* (NHMUK 2571), the femoral head is less projected medially than in GSN R327 as seen in ventral view. In *Cynognathus* (NHMUK 2571), the lesser trochanter is straight and centered on the ventral surface of the femur, whereas it is curved and relatively displaced medially in GSN R327.

In *?Aleodon/?Scalenodon* (NHMUK 8; Jenkins, 1971; Liu et al., 2017:fig. 15C), the femur has a slender diaphysis and a more rounded proximal margin as seen dorsally, when compared with GSN R327.

The femoral head of *Exaeretodon argentinus* is more conspicuous and more expanded dorsoventrally than in GSN R327 (Bonaparte, 1963; Liu et al., 2017:fig. 15K–L). The lesser trochanter of *E. argentinus* is more robust than in GSN R327 and, in medial view, its outline is concave, whereas in GSN R327 it is crest-like and convex. The lesser trochanter is on the medial margin of the bone in *Exaeretodon*, unlike what is observed in GSN R327. A crest connected to the greater trochanter on the ventral surface of the femur of *E. argentinus*, interpreted to be the third trochanter (Bonaparte, 1963), is not present in GSN R327.

Unlike the almost straight femur of GSN R327, in *Pascualgnathus* the proximal portion of the femur is strongly curved laterally (Bonaparte, 1966; Liu et al., 2017:fig. 15A–B). The femoral head appears as relatively less projected medially in *Pascualgnathus* than in GSN R327. The greater trochanter is poorly developed dorsoventrally in *Pascualgnathus* when compared with GSN R327. In medial view, the external margin of the lesser trochanter is straight in *Pascualgnathus*, whereas it is convex in GSN R327.

When compared with GSN R327, the femoral head of *Cricodon* is more proximally projected relative to the greater trochanter (see Crompton, 1955).

In *Traversodon* (Huene, 1935–1942:pl. 16.3a, b), the greater trochanter is more distally placed with respect to the femoral head, which is more robust and more medially projected than in GSN R327. In ventral view, the femur of *Traversodon* is sigmoid, whereas that of GSN R327 is approximately straight.

In ventral view, the femur of *Massetognathus pascuali* (Jenkins, 1971; PVL 5444; PVL S/N) has a better-defined and more laterally projecting greater trochanter, a lesser trochanter that is more robust, more distally placed, and more projecting medially, and a better developed and more proximally (not so medially) directed femoral head than in GSN R327. In *M. pascuali* specimen MCZ 3801, the greater trochanter is proximally (not so laterally) projected and very robust when compared with GSN R327. In the femur of *M. ochagaviae* (see Pavanatto et al., 2016), the lesser trochanter is not so projected medially and not so distally placed as in *M. pascuali* specimens.

In *Luangwa drysdalli*, the femoral head projects more proximally and is more bowed dorsally than in GSN R327 (in which it is mainly medially projecting) and the lesser trochanter is a medially directed, flange-like structure, whereas in GSN R327 there is

only a low crest on the ventral face of the femur (Kemp, 1980; Liu et al., 2017:fig. 15D).

Unlike in GSN R327, in *Andescynodon* the lesser trochanter is a medially directed flange. The greater trochanter in *Andescynodon* is more distally placed (relative to the femoral head) than in GSN R327. The published femur of *Andescynodon* is only poorly preserved (Liu and Powell, 2009), precluding further comparisons with GSN R327.

The femur of *Boreogomphodon* is similar to that of GSN R327, only differing in the more elongated femoral neck and in the relatively laterally placed lesser trochanter on the ventral surface of the bone.

Fibula

The fibula of GSN R327 differs in many respects from the type I and II fibulae of *?Cynognathus/?Diademodon* (Jenkins, 1971).

In *?Cynognathus/?Diademodon* (BPI 1675; Jenkins, 1971), the fibular tubercle appears to have been better developed than that of GSN R327. Medially, there is an oval depression between the fibular tubercle and the medial ridge in GSN R327 that is absent in BPI 1675, where there is a deep and narrow groove instead. Laterally, on the proximal third of the fibula, the posterolateral ridge observed in GSN R327 is shorter and more robust than the one in BPI 1675. The groove at mid-length of the diaphysis observed anteriorly in the fibula BPI 1675 is absent in GSN R327.

The fibula of *Exaeretodon argentinus* and *Traversodon* is more robust and is relatively more expanded distally and proximally than that of GSN R327 (Huene, 1935–1942; Bonaparte, 1963), whereas this bone is more robust and the proximal portion is more expanded in GSN R327 than in *Pascualgnathus* (Bonaparte, 1966). Unlike in GSN R327, the fibula is more compressed mediolaterally than anteroposteriorly in *E. argentinus*.

In *Massetognathus pascuali* (PVL 5444, PVL 4442, MCZ 3801, MCZ 4018), the fibula is more gracile than that of GSN R327. The fibula of *M. pascuali* MCZ 3801 is straight, which is different not only from GSN R327 but also from other *M. pascuali* specimens, in which this bone is curved. A groove along the medial surface of the fibula is present in *M. pascuali* but not in GSN R327.

Lumbar Rib

The preserved lumbar rib of GSN R327 is very similar in outline to those of *Diademodon* specimen NMQR 531 (Brink, 1955: fig. 4), *Microgomphodon eumerus* (NHMUK 3581; Seeley, 1895a; *Diademodon* according to Brink, 1955), *?Cynognathus/?Diademodon* (BPI 1675; Jenkins, 1971), and *Cynognathus* (NHMUK 2571; Seeley, 1895b; Jenkins, 1971).

In *Diademodon* specimen NMQR 531, *?Cynognathus/?Diademodon* (BPI 1675), and *Cynognathus* (NHMUK 2571), the dorsal ridge is medially placed, whereas it is centered on the expanded portion of the lumbar rib in GSN R327. *Cynognathus* (NHMUK 2571) and *?Cynognathus/?Diademodon* (BPI 1675) differ from GSN R327 in the more laterally reflected dorsal ridge and in the presence of facets for adjacent ribs. The articulated ribs of NHMUK 3581 are only exposed ventrally; thus, it is not possible to ascertain the presence of facets for adjacent ribs and the characteristics of the dorsal ridge.

In *Pascualgnathus* (Bonaparte, 1963) and SAM-PK-K4002, the preserved lumbar ribs are only observable in ventral view. They have a triangular outline, with the neck of the rib expanding gradually laterally, differing from the abrupt expansion of the rib in GSN R327.

Unlike GSN R327, *Luangwa* (Kemp, 1980) shares with *Pascualgnathus* and SAM-PK-K4002 the general outline of the lumbar ribs and the dorsal ridge is posteriorly positioned and directed obliquely.

The preserved lumbar ribs of *Traversodon* (Huene, 1935–1942: pl. 17.4–8) differ in outline and in the orientation of the dorsal ridge from those of GSN R327.

Unlike in GSN R327, the expanded portion of the lumbar ribs of *Massetognathus pascuali* is not plate-like.

DISCUSSION

According to the observations presented above, *Diademodon* can be distinguished from other cynognathians on the basis of its postcranial anatomy. Particularly, the comparisons presented here show that there are several postcranial features that allow us to differentiate *Diademodon* specimen GSN R327 from other specimens previously assigned to this genus and from *Cynognathus* individuals. In this context, some significant postcranial features identified in GSN R327 can be used to diagnose *Diademodon*.

Apart from GSN R327, the postcranial remains of *Gomphognathus* (= *Diademodon*) specimen AM 458 (Broom, 1903), specimen SAM-PK-K5266 (Gow and Grine, 1979), and SAM-PK-K4002 (Abdala, 1999) are the only ones in the literature to date that can be unambiguously identified as *Diademodon*. Regarding AM 458 (Broom, 1903), our comparisons are restricted to the fused condition of the atlas and axis centra shared by this specimen and GSN R327. Specimen SAM-PK-K5266 is poorly preserved, and only a short account of its postcranial anatomy without detailed illustrations was published (Gow and Grine, 1979). Comparisons between SAM-PK-K5266 and GSN R327 are restricted to the interclavicle. This bone is similar in SAM-PK-K5266 and GSN R327, differing in a few minor features such as the shape of the posterior margin and the presence/absence of ventral striations on the posterior region of the bone. The partially preserved humerus of SAM-PK-K4002 is similar to that of GSN R327, whereas the recovered lumbar ribs differ from those of GSN R327.

Brink (1955) presented an account of *Diademodon*, describing cranial as well as postcranial material on the basis of many specimens. However, the unambiguous attribution of the postcranial elements (including an articulated partial skeleton, NMQR 531) described by Brink to the genus *Diademodon* is not possible (see also Jenkins, 1971:75). Comparisons between these specimens and *Diademodon tetragonus* specimen GSN R327 highlight differences in the axis (GSN R202 and GSN R205), scapula (GSN R224), and also in the fused/unfused condition of the postaxial cervical intercentra (GSN R227). Additionally, although not properly figured, the ilium described by Brink (1955; collection number not specified, probably NMQR 531) differs notably in the shape of the anterior margin from the ilium preserved in GSN R327. The lumbar ribs of NMQR 531 also differ from those of GSN R327. The dissimilarities recognized suggest that Brink's specimens do not belong to the same taxon as GSN R327. In this context, either Brink's generic determination of the specimens is incorrect (i.e., they must belong to another genus) or it is correct and the differences can be attributed to interspecific variability (i.e., there is more than one species of *Diademodon*).

Originally described as *Microgomphodon eumerus* by Seeley (1895a), NHMUK 3581 was later interpreted to be a small specimen of *Diademodon* (Brink, 1955:31; see also Jenkins, 1971) on the basis of the published illustrations. From these illustrations, it can be concluded that, in general terms, what is visible of the femur, ilium, and lumbar ribs of NHMUK 3581 (see Seeley, 1895a:pl. 1) is comparable to the morphology observed in GSN R327. On the other hand, the proximal portion of the humerus of NHMUK 3581 is much more expanded mediolaterally than in GSN R327. In this scenario, it is possible that Seeley's specimen (NHMUK 3581) may in fact represent a tiny *Diademodon* specimen, as suggested by Brink (1955), and the differences in the humerus could be attributed to changes throughout ontogeny.

However, this statement should be taken with caution until stronger evidence is provided.

Seeley (1895a) also described and illustrated a humerus that he referred to *Gomphognathus*, a taxon later synonymized with *Diademodon* (Brink, 1955; Watson and Romer, 1956). The assignment of this specimen to *Diademodon* is doubtful (see Jenkins, 1971), a fact also suggested by several differences recognized here with GSN R327.

Abdala (1999) compared the humerus of a South American *Cynognathus* specimen (PVL 3859) with specimens NHMUK 3772a and NMB C2693 described by Watson (1917) and Jenkins (1971), respectively. Due to differences in the morphology of the humeral head, development of the proximal and distal ends, and the morphology of the deltopectoral crest, Abdala (1999) concluded that the specimens described by the latter authors more likely belonged to *Diademodon*. Our analysis shows that the available elements of NHMUK 3772a (i.e., interclavicle and humerus) differ in several aspects from GSN R327, suggesting that NHMUK 3772a might represent a taxon different from *Diademodon tetragonus*.

In his monographic work on the postcranial skeleton of African cynodonts, Jenkins (1971) analyzed a number of specimens that he referred to as *?Cynognathus/?Diademodon*. Among them, the clavicle (NMB C2700), the scapula (NMB C2711), ulna (BPI 1695), radius (BPI 1695), ilium (BPI 1695), ischium (NMB C2702), type I and II fibulae (BPI 1675), and lumbar ribs (BPI 1675) differ from those elements in specimen GSN R327, unambiguously identified as *Diademodon tetragonus*. This suggests that Jenkins' specimens (NMB C2700, NMB C2711, NMB C2702, BPI 1675, and BPI 1695) are not *Diademodon*. Whether these specimens can be assigned to *Cynognathus* is beyond the scope of the present study and requires detailed comparisons with postcranial remains unambiguously assigned to that taxon. On the other hand, the femur (NMB C2694) and humerus (NMB C2693) tentatively assigned to *?Cynognathus/?Diademodon* as presented by Jenkins (1971) are similar to those of GSN R327. Although there are some differences, most of them are interpreted to be related to muscle development and insertion and could be attributed to interspecific variation. Hence, specimens NMB C2693 and NMB C2694 may indeed be assignable to *Diademodon*, in concordance with what was suggested for NMB C2693 by Abdala (1999).

Jenkins (1971) also described some postcranial elements of *Cynognathus* (NHMUK 2571; see also Seeley, 1895b) and the interclavicle of an undetermined cynognathian DMSW R 435. When compared with GSN R327, *Cynognathus* specimen NHMUK 2571 is very similar regarding the morphology of the cervical vertebrae, only differing in the relative position of the transverse processes of the axis. On the other hand, these specimens show conspicuous differences in the ischium and lumbar ribs. The interclavicle of the undetermined cynognathian (DMSW R 435) differs from that of GSN R327; hence, we propose tentatively that DMSW R 435 cannot be assigned to *Diademodon*.

Our study suggests that in the best scenario, only a few specimens of *Diademodon* are known (Table 1). Most of these specimens consist of isolated bones, and only two are partially articulated skeletons. Among the latter, one specimen is not fully prepared (NHMUK 3581) and the other is poorly preserved (NMQR 531). Specimen GSN R327 is the most complete and best-preserved specimen unambiguously assignable to *Diademodon tetragonus* known to date.

The presence of an ossified sternum has been only reported in tritylodontids among non-mammaliaform cynodonts (Kühne, 1956; Sun and Li, 1985; Sues and Jenkins, 2006). Considering the large representation of cynognathian specimens, many of them very well preserved, the general absence of sternal elements suggests that they were cartilaginous, precluding fossilization. In

TABLE 1. Taxonomic identification of possible *Diademodon* specimens.

Specimen	Main reference	Elements analyzed	Previous identification	Identification (this paper)
SAM-PK-K4002	Abdala, 1999	Humerus, vertebrae, lumbar rib	<i>Diademodon</i>	<i>D. tetragonus</i>
GSN R202, GSN R205	Brink, 1955	Atlas-axis centrum	<i>Diademodon</i>	not <i>D. tetragonus</i>
GSN R224	Brink, 1955	Scapula	<i>Diademodon</i>	not <i>D. tetragonus</i>
GSN R227	Brink, 1955	Postaxial cervical vertebrae	<i>Diademodon</i>	not <i>D. tetragonus</i>
NMQR 531	Brink, 1955	Ilium, lumbar rib	<i>Diademodon</i>	not <i>D. tetragonus</i>
AM 458	Broom, 1903	Atlas-axis centrum	<i>Diademodon</i>	<i>D. tetragonus</i>
SAM-PK-K5266	Gow and Grine, 1979	Interclavicle	<i>Diademodon</i>	<i>D. tetragonus</i>
BPI 1675	Jenkins, 1971	Fibula, lumbar rib	? <i>Cynognathus</i> / <i>Diademodon</i>	not <i>D. tetragonus</i>
BPI 1695	Jenkins, 1971	Ulna, radius, ilium	? <i>Cynognathus</i> / <i>Diademodon</i>	not <i>D. tetragonus</i>
NMB C2700	Jenkins, 1971	Clavicle	? <i>Cynognathus</i> / <i>Diademodon</i>	not <i>D. tetragonus</i>
NMB C2702	Jenkins, 1971	Ischium	? <i>Cynognathus</i> / <i>Diademodon</i>	not <i>D. tetragonus</i>
NMB C2711	Jenkins, 1971	Scapula	? <i>Cynognathus</i> / <i>Diademodon</i>	not <i>D. tetragonus</i>
NMB C2693	Jenkins, 1971	Humerus	? <i>Cynognathus</i> / <i>Diademodon</i>	<i>D. tetragonus</i>
NMB C2694	Jenkins, 1971	Femur	? <i>Cynognathus</i> / <i>Diademodon</i>	<i>D. tetragonus</i>
DMSW R 435	Jenkins, 1971	Interclavicle	Unidentified cynognathian	not <i>D. tetragonus</i>
NHMUK 3581	Seeley, 1895a	Femur, ilium, humerus, lumbar rib	<i>Diademodon</i>	<i>D. tetragonus</i>
NHMUK R2579	Seeley, 1895a:figs. 12–13	Humerus	<i>Diademodon</i>	not <i>D. tetragonus</i>
NHMUK 3772a	Watson, 1917	Interclavicle, humerus	<i>Diademodon</i>	not <i>D. tetragonus</i>

this context, the finding of an ossified manubrium and two sternebra in the Namibian specimen of *Diademodon* described here (GSN R327) stands out as a unique feature of this genus among cynognathians. The scarce information regarding *Diademodon* postcranial anatomy to date makes it possible that an ossified sternum has remained unrecognized by previous authors.

The presence of an ossified sternum in *Diademodon* cannot be attributed to the relatively large body size reached by individuals of this taxon. In the cynognathian lineage, *Cynognathus* and *Exaeretodon argentinus* are among the largest non-mammaliaform cynodonts, but in neither of them has an ossified sternum been described up to now. Furthermore, among tritylodontids, an ossified sternum is present in small (*Bienotheroides* and *Oligokyphus*) and large (*Kayentatherium*) forms, suggesting that its presence is not related to body size and could be a phylogenetically informative trait. Hence, it is proposed here that the presence of an ossified sternum in addition to an interclavicle should be considered a diagnostic character of *Diademodon*. The absence of this feature in taxa closely related to *Diademodon* precludes inferences regarding its phylogenetic implications.

CONCLUSIONS

Diademodon tetragonus is a relatively large basal cynognathian, known from several specimens found in Triassic localities of southern Africa and Argentina. A number of postcranial remains have tentatively been assigned to this taxon; however, only four specimens include diagnostic cranial material associated with postcranial elements. One of these specimens (USNM V23352) has never been published, and, according to Jenkins (1971), its postcranial remains are not very informative. The postcranium of other specimens (AM 458, SAM-PK-K5266, SAM-PK-K4002) is only poorly represented, and only a few elements could be compared with the Namibian specimen described here (GSN R327).

Among the specimens lacking diagnostic elements, NHMUK 358 was originally identified as *Microgomphodon eumerus* (see Seeley, 1895a) and then reinterpreted as a small individual of *Diademodon* (Brink, 1955; Jenkins, 1971). We agree with the latter view because there are many shared traits between NHMUK 3581 and GSN R327, interpreting that the differences observed are in response to ontogenetic changes. The assignment of other specimens to *Diademodon* is not supported by our comparative morphological analysis. Regarding the specimens described as ?*Cynognathus*?/*Diademodon* by Jenkins (1971), only some of them (i.e., the femur NMB C2694 and the humerus NMB C2693)

likely belong to *Diademodon*, whereas the others (NMB C2711, NMB C2702, and BPI 1695) must be regarded as a different taxon. Hence, our study highlights that there are only a few published specimens including postcranial elements that can be identified as *Diademodon*.

Contrary to the generally held view that the postcranial skeleton of cynognathian cynodonts is mostly conservative (e.g., Jenkins, 1971), our analysis also shows that several postcranial features distinguish *Diademodon* from other cynognathians. The most conspicuous of these differences is the presence of an ossified manubrium and sternebrae, which is identified as a unique feature of *Diademodon tetragonus* among cynognathians and is not related to its relatively large body size, but could be of phylogenetic value.

ACKNOWLEDGMENTS

We are grateful to M. Raath and B. Zipfel (Evolutionary Studies Institute, University of the Witwatersrand), the late J. Powell (Instituto Miguel Lillo), J. Cundiff (Museum of Comparative Zoology, Harvard University), and Geological Survey of Namibia authorities for granting access to the collections under their care. The editor (Dr. T. Martin) and reviewers (Dr. J. Fröbisch and Dr. A. Martinelli) are thanked for their useful comments, which greatly improved the manuscript.

This research article was possible thanks to funding provided by the National Research Foundation of South Africa and the National Research Foundation Research Incentive to F.A.; Programa de Viajes Internacionales de la Universidad de Buenos Aires, PICT 2013–2701, and PIP 11220150100760CO to L.C.G.; PICT 2014–1921 to V. Krapovic; and the Bi-National Cooperation Project between South Africa (Department of Science and Technology to B. Rubidge) and Argentina (Ministerio de Ciencia, Técnica e Innovación Productiva to C. Marsicano). This is L. C.G.'s R-231 contribution to the IDEAN.

FUNDING

This work was supported by Consejo Nacional de Investigaciones Científicas y Técnicas (11220150100760CO); Fondo para la Investigación Científica y Tecnológica (2013–2701, PICT 2014–1921); Ministerio de Ciencia, Tecnología e Innovación Productiva (Bi-National Cooperation Project between South Africa); National Research Foundation Research Incentive; National Research Foundation of South Africa; Universidad de Buenos Aires (Programa de Viajes Internacionales).

LITERATURE CITED

- Abdala, F. 1999. Elementos postcraneanos de *Cynognathus* (Synapsida-Cynodontia) del Triásico Inferior de la Provincia de Mendoza, Argentina. Consideraciones sobre la morfología del húmero en cinodontes. *Revista Española de Paleontología* 14:13–24.
- Abdala, F., and R. M. H. Smith. 2009. A middle Triassic cynodont fauna from Namibia and its implications for the biogeography of Gondwana. *Journal of Vertebrate Paleontology* 29:837–851.
- Abdala, F., P. J. Hancox, and J. Neveling. 2005. Cynodonts from the uppermost Burgersdorp Formation, South Africa, and their bearing on the biostratigraphy and correlation of the Triassic *Cynognathus* Assemblage Zone. *Journal of Vertebrate Paleontology* 25:192–199.
- Abdala, F., C. A. Marsicano, R. H. M. Smith, and R. Swart. 2013. Strengthening western Gondwanan correlations: a Brazilian dicynodont (Synapsida, Anomodontia) in the Middle Triassic of Namibia. *Gondwana Research* 23:1151–1162.
- Bonaparte, J. F. 1963. Descripción del esqueleto postcraneano de *Exaeretodon*. *Acta Geológica Lilloana* 4:5–52.
- Bonaparte, J. F. 1966. Una nueva “fauna” Triásica de Argentina. (Therapsida: Cynodontia–Dicynodontia). Consideraciones filogenéticas y paleobiogeográficas. *Ameghiniana* 4:243–296.
- Botha, J., and A. Chinsamy. 2000. Growth patterns deduced from the bone histology of the cynodonts *Diademodon* and *Cynognathus*. *Journal of Vertebrate Paleontology* 20:705–711.
- Botha, J., J. Lee-Thorp, and A. Chinsamy. 2005. The palaeoecology of the non-mammalian cynodonts *Diademodon* and *Cynognathus* from the Karoo Basin of South Africa, using stable light isotope analysis. *Palaeogeography, Palaeoclimatology, Palaeoecology* 223:303–316.
- Bradu, D., and F. E. Grine. 1979. Multivariate analysis of *Diademodon* crania from South Africa and Zambia. *South African Journal of Science* 75:441–448.
- Brink, A. S. 1955. A study on the skeleton of *Diademodon*. *Palaeontologia africana* 3:3–39.
- Brink, A. S. 1956. Speculations on some advanced mammalian characteristics in the higher mammal-like reptiles. *Palaeontologia africana* 4:77–96.
- Brink, A. S. 1963. Notes on some *Diademodon* specimens in the collection of the Bernard Price Institute. *Palaeontologia africana* 8:97–111.
- Brink, A. S. 1979. Genera and species of the Diademodontinae. *Bulletin of the Geological Survey of South Africa* 65:1–50.
- Broili, F., and J. Schröder. 1935. Beobachtungen an Wirbeltieren der Karooformation. IX Über den Schädel von *Gomphognathus* Seeley. *Sitzungsberichte der Bayerischen Akademie der Wissenschaften* 1935:115–182.
- Broom, R. 1903. On the axis, atlas and proatlas in the higher theriodonts. *Proceedings of the Zoological Society of London* 73:177–180.
- Broom, R. 1905. On the use of the term Anomodontia. *Records of the Albany Museum* 1:266–269.
- Broom, R. 1911. On the structure of the skull in cynodont reptiles. *Proceedings of the Zoological Society of London* 81:893–925.
- Broom, R. 1919. On the genus *Gomphognathus* and its allies. *Records of the Albany Museum* 3:223–232.
- Crompton, A. W. 1955. On some Triassic cynodont from Tanganyika. *Proceedings of the Zoological Society of London* 125:617–669.
- Crompton, A. W. 1972. Postcanine occlusion in cynodonts and tritylodonts. *Bulletin of the British Museum (Natural History), Geology* 21:29–71.
- Ezcurra, M. D., L. E. Fiorelli, A. G. Martinelli, S. Rocher, M. B. von Baczko, M. Ezpeleta, J. R. A. Taborda, E. M. Hechenleitner, M. J. Trotteyn, and J. B. Desojo. 2017. Deep faunistic turnovers preceded the rise of dinosaurs in southwestern Pangaea. *Nature Ecology and Evolution* 1:1477–1483. doi: 10.1038/s41559-017-0305-5.
- Fourie, S. 1963. Tooth replacement in the gomphodont cynodont *Diademodon*. *South African Journal of Science* 59:211–213.
- Gow, C. E., and F. E. Grine. 1979. An articulated skeleton of a small individual of *Diademodon* (Therapsida: Cynodontia). *Palaeontologia africana* 22:29–34.
- Grine, F. E. 1977. Postcanine tooth function and jaw movement in the gomphodont cynodont *Diademodon* (Reptilia; Therapsida). *Palaeontologia africana* 20:123–135.
- Grine, F. E. 1978. Notes on a specimen of *Diademodon* previously referred to as *Cyclogomphodon*. *Palaeontologia africana* 21:167–174.
- Grine, F. E. 1981. *Cragievarus kitchingi* Brink, 1965: a subjective junior synonym of *Diademodon tetragonus* Seeley, 1894 (Reptilia, Therapsida). *Annals of the South African Museum* 84:151–168.
- Grine, F. E., and B. D. Hahn. 1978. Allometric growth in the Diademodontinae (Reptilia; Therapsida): a preliminary report. *Palaeontologia africana* 21:161–166.
- Grine, F. E., B. D. Hahn, and C. E. Gow. 1978. Aspect of relative growth and variability in *Diademodon* (Reptilia; Therapsida). *South African Journal of Science* 74:50–58.
- Grine, F. E., D. Mitchell, C. E. Gow, J. W. Kitching, and B. R. Turner. 1979. Evidence for salt glands in the Triassic reptile *Diademodon* (Therapsida; Cynodontia). *Palaeontologia africana* 22:35–39.
- Holzförster, F., H. Stollhofen, and I. G. Stanistreet. 1999. Lithostratigraphy and depositional environments in the Waterberg-Erongo area, central Namibia, and correlation with the main Karoo Basin, South Africa. *Journal of African Earth Sciences* 29:105–123.
- Hopson, J. A. 1971. Postcanine replacement in the gomphodont cynodont *Diademodon*; pp. 1–21 in D. M. Kermack and K. A. Kermack (eds.), *Early Mammals*. *Zoological Journal of the Linnean Society* 50(Supplement 1).
- Hopson, J. A., and J. W. Kitching. 1972. A revised classification of cynodonts (Reptilia, Therapsida). *Palaeontologia africana* 14:71–85.
- Hopson, J. A., and J. W. Kitching. 2001. A probainognathian cynodont from South Africa and the phylogeny of non-mammalian cynodonts. *Bulletin of the Museum of Comparative Zoology* 156:5–35.
- Huene, F. von. 1935–1942. pp. 93–159 in *Die fossilen Reptilien des südamerikanischen Gondwanalandes*. 2. Ordnung Cynodontia. C. H. Beck, Munich.
- Jenkins, F. A., Jr. 1970. The Chañares (Argentina) Triassic reptile fauna VII. The postcranial skeleton of the traversodontid *Massetognathus pascuali* (Therapsida, Cynodontia). *Breviora* 352:1–28.
- Jenkins, F. A., Jr. 1971. The postcranial skeleton of African cynodonts. *Bulletin of the Peabody Museum of Natural History* 36:1–216.
- Kammerer, C. F., J. J. Flynn, L. Ranivoharimanana, and A. R. Wyss. 2008. New material of *Menadon besairiei* (Cynodontia: Traversodontidae) from the Triassic of Madagascar. *Journal of Vertebrate Paleontology* 28:445–462.
- Kemp, T. S. 1980. Aspect of the structure and functional anatomy of the Middle Triassic cynodont *Luangwa*. *Journal of Zoology* 191:193–239.
- Kemp, T. S. 1982. *Mammal-like Reptiles and the Origin of Mammals*. Academic Press, London, 363 pp.
- Keyser, A. W. 1973a. A new Triassic vertebrate fauna from South West Africa. *Palaeontologia africana* 16:1–15.
- Keyser, A. W. 1973b. New Triassic vertebrate fauna from South West Africa. *South African Journal of Science* 69:113–115.
- Keyser, A. W. 1978. A new bauriamorph from the Omingonde Formation (Middle Triassic) of South West Africa. *Palaeontologia africana* 21:177.
- Kitching, J. W. 1995. Biostratigraphy of the *Cynognathus* Assemblage Zone; pp. 40–45 in B. S. Rubidge (ed.), *Biostratigraphy of the Beaufort Group (Karoo Supergroup)*. Series 1. South African Committee for Stratigraphy, Pretoria, South Africa.
- Kühne, W. G. 1956. The Liassic Therapsid *Oligokyphus*. *British Museum of Natural History, London*, 149 pp.
- Liu, J., and F. Abdala. 2014. Phylogeny and taxonomy of the Traversodontidae; pp. 255–279 in C. F. Kammerer, K. D. Angielczyk, and J. Fröbisch (eds.), *Early Evolutionary History of the Synapsida*. Springer, Dordrecht, The Netherlands.
- Liu, J., and P. Olsen. 2010. The phylogenetic relationships of Eucynodontia (Amniota: Synapsida). *Journal of Mammalian Evolution* 17:151–176.
- Liu, J., and J. Powell. 2009. Osteology of *Andescynodon* (Cynodontia: Traversodontidae) from the Middle Triassic of Argentina. *American Museum Novitates* 3674:1–19.
- Liu, J., V. P. Schneider, and P. E. Olsen. 2017. The postcranial skeleton of *Boreogomphodon* (Cynodontia: Traversodontidae) from the Upper Triassic of North Carolina, USA and the comparison with other traversodontids. *PeerJ* 5:e3521. doi: 10.7717/peerj.3521.
- Liu, J., M. B. Soares, and M. Reichel. 2008. *Massetognathus* (Cynodontia, Traversodontidae) from the Santa Maria Formation of Brazil. *Revista Brasileira de Paleontologia* 11:27–36.

- Marsicano, C. A., R. B. Irmis, A. C. Mancuso, R. Mundil, and F. Chemale. 2016. The precise temporal calibration of dinosaur origins. Proceedings of the National Academy of Sciences of the United States of America 113:509–513.
- Martinelli, A. G., M. de la Fuente, and F. Abdala. 2009. *Diademodon tetragonus* (Therapsida: Cynodontia) in the Triassic of South America and its biostratigraphic implications. Journal of Vertebrate Paleontology 29:852–862.
- Martinelli, A. G., C. F. Kammerer, T. P. Melo, V. D. Paes Neto, A. M. Ribeiro, Á. A. S. Da-Rosa, C. L. Schultz, and M. Bento Soares. 2017. The African cynodont *Aleodon* (Cynodontia, Probainognathia) in the Triassic of southern Brazil and its biostratigraphic significance. PLoS ONE 12:e0177948. doi: 10.1371/journal.pone.0177948.
- Oliveira, T. V., C. L. Schultz, and M. Bento Soares. 2007. O esqueleto pós-craniano de *Exaeretodon riograndensis* Abdala et al. (Cynodontia, Traversodontidae), Triássico do Brasil. Revista Brasileira de Paleontologia 10:79–94.
- Osborn, J. W. 1974. On tooth succession in *Diademodon*. Evolution 28:141–157.
- Ottone, E. A., M. Monti, C. A. Marsicano, M. de la Fuente, M. Naipauer, R. Armstrong, and A. C. Mancuso. 2014. A new Late Triassic age for the Puesto Viejo Group (San Rafael depocenter, Argentina): SHRIMP U–Pb zircon dating and biostratigraphic correlations across southern Gondwana. Journal of South American Earth Sciences 56:186–199.
- Owen, R. 1861. Palaeontology, or a systematic summary of extinct animals and their geological relations. Adam and Charles Buck, Edinburgh.
- Pavanatto, A. E. B., R. T. Müller, Á. A. S. Da-Rosa, and S. Dias-da-Silva. 2016. New information on the postcranial skeleton of *Massetognathus ochagaviae* Barberena, 1981 (Eucynodontia, Traversodontidae), from the Middle Triassic of Southern Brazil. Historical Biology 28:978–989.
- Seeley, H. G. 1894. Research on the structure, organization, and classification of the Fossil Reptilia. Part IX, Section 3. On *Diademodon*. Philosophical Transactions of the Royal Society of London 185:1029–1041.
- Seeley, H. G. 1895a. Researches on the structure, organization and classification of the fossil Reptilia. Pt. IX, Sect. 4. On the Gomphodontia. Philosophical Transactions of the Royal Society of London Series B 186:1–57.
- Seeley, H. G. 1895b. Researches on the structure, organization and classification of the fossil Reptilia. Pt. IX, Sec. 5. On the skeleton in new Cynodontia from the Karoo Rocks. Philosophical Transactions of the Royal Society of London Series B 186:59–148.
- Smith, R. M. H., and R. Swart. 2002. Changing fluvial environments and vertebrate taphonomy in response to climatic drying in a Mid-Triassic rift valley fill: the Omingonde Formation (Karoo Supergroup) of central Namibia. Palaios 17:249–267.
- Smith, R. M. H., B. Rubidge, and M. van der Walt. 2012. Therapsid biodiversity patterns and palaeoenvironments of the Karoo Basin, South Africa; pp. 30–62 in A. Chinsamy-Turan (ed.), Forerunners of Mammals. Indiana University Press, Bloomington, Indiana.
- Sues, H.-D., and F. A. Jenkins Jr. 2006. The postcranial skeleton of *Kayentatherium wellsi* from the Lower Jurassic Kayenta Formation of Arizona and the phylogenetic significance of the postcranial features of tritylodontid cynodonts; pp. 114–152 in M. T. Carrano, T. J. Gaudin, R. W. Blob, and J. R. Wible (eds.), Amniote Paleobiology. Perspectives on the Evolution of Mammals, Birds and Reptiles. Chicago University Press, Chicago, Illinois.
- Sun, A., and Y. Li. 1985. The postcranial skeleton of the late tritylodont *Bienotheroides*. Vertebrata Palasiatica 23:133–151. [Chinese with English summary].
- Wanke, A. 2000. Karoo-Etendeka unconformities in NW Namibia and their tectonic implications. Ph.D. dissertation, Bayerischen Julius-Maximilians-Universität, Würzburg, Germany, 114 pp.
- Watson, D. M. S. 1911. The skull of *Diademodon*, with notes on those of some other cynodonts. The Annals and Magazine of Natural History (series 8) 8:293–330.
- Watson, D. M. S. 1913. Further notes on the skull, brain, and organs of special sense of *Diademodon*. The Annals and Magazine of Natural History (series 8) 12:217–228.
- Watson, D. M. S. 1917. The evolution of the tetrapod shoulder girdle and forelimb. Journal of Anatomy 52:1–63.
- Watson, D. M. S., and A. S. Romer. 1956. A classification of therapsid reptiles. Bulletin of the Museum of Comparative Zoology 114:37–89.

Submitted September 1, 2017; revisions received December 21, 2017; accepted January 3, 2018.

Handling editor: Thomas Martin.